3-28-1972

Continuous Wave Co2 Laser Degradation And Mass Spectrometric Analysis Of Organic Polymers.

Stanley G. Coloff

THE UNIVERSITY OF NEW MEXICO
ALBUQUERQUE, NEW MEXICO 87106

Policy on Use of Theses and Dissertations

Unpublished theses and dissertations accepted for master's and doctor's degrees and deposited in the University of New Mexico Library are open to the public for inspection and reference work. *They are to be used only with due regard to the rights of the authors.* The work of other authors should always be given full credit. Avoid quoting in amounts, over and beyond scholarly needs, such as might impair or destroy the property rights and financial benefits of another author.

To afford reasonable safeguards to authors, and consistent with the above principles, anyone quoting from theses and dissertations must observe the following conditions:

1. Direct quotations during the first two years after completion may be made only with the written permission of the author.

2. After a lapse of two years, theses and dissertations may be quoted without specific prior permission in works of original scholarship provided appropriate credit is given in the case of each quotation.

3. Quotations that are complete units in themselves (e.g., complete chapters or sections) in whatever form they may be reproduced and quotations of whatever length presented as primary material for their own sake (as in anthologies or books of readings) ALWAYS require consent of the authors.

4. The quoting author is responsible for determining "fair use" of material he uses.

This thesis/dissertation by Stanley G. Coloff has been used by the following persons whose signatures attest their acceptance of the above conditions. (A library which borrows this thesis/dissertation for use by its patrons is expected to secure the signature of each user.)

NAME AND ADDRESS	DATE

July 1971—1,000—GS

This thesis, directed and approved by the candidate's committee, has been accepted by the Graduate Committee of The University of New Mexico in partial fulfillment of the requirements for the degree of

Master of Science in Chemistry

CONTINUOUS WAVE CO_2 LASER DEGRADATION AND MASS SPECTROMETRIC ANALYSIS OF ORGANIC POLYMERS

Title

Stanley G. Coloff

Candidate

Chemistry

Department

Charles L. Berkel

Dean

March 25, 1972

Date

Committee

Nicholas E. Vandeborgh

Chairman

Roy Eaton, Jr.

Edward A. Walters

Guido H. Daub

CONTINUOUS WAVE CO_2 LASER DEGRADATION AND MASS SPECTROMETRIC ANALYSIS OF ORGANIC POLYMERS

BY

Stanley G. Coloff

THESIS

Submitted in Partial Fulfillment of the
Requirements for the Degree of
Master of Science in Chemistry
in the Graduate School of
The University of New Mexico
Albuquerque, New Mexico

January, 1972

ACKNOWLEDGEMENTS

The author is very grateful for the use of equipment and facilities of the Laser Division and Scientific Support Branch of the Air Force Weapons Laboratory.

A deep debt of gratitude is due Mr. Wayne Wasson and Mr. Willey Knuzler of the Air Force Weapons Laboratory for their technical assistance throughout the project. Acknowledgement is due Dr. A. Guenther and Sister Rosalie Urzendowski also of the Air Force Weapons Laboratory.

The timely discussions with Dr. Ken Lincoln of NASA, Ames Research Center were greatly appreciated.

Special gratitude is due Dr. N. E. Vanderborgh of the University of New Mexico for his confidence, support and continued encouragement in this project.

A very special thanks to my wife for her patience and courage.

CONTINUOUS WAVE CO_2 LASER DEGRADATION AND MASS SPECTROMETRIC ANALYSIS OF ORGANIC POLYMERS

BY

Stanley G. Coloff

ABSTRACT OF THESIS

Submitted in Partial Fulfillment of the
Requirements for the Degree of
Master of Science in Chemistry
in the Graduate School of
The University of New Mexico
Albuquerque, New Mexico

January, 1972

ABSTRACT

Previous laser-mass spectrometer and laser-gas-chromatographic instruments for study of organic polymer degradation have used high power pulsed lasers (ruby, Nd-glass) which limit sample characterization due to extensive fragmentation.

A new experimental technique has been developed for high temperature pyrolysis and rapid analysis of organic polymers. The experimental technique combines a low power continuous wave CO_2 laser for sample pyrolysis and a time-of-flight mass spectrometer to analyze degradation products. The laser built for use in this study was a continuous flow CO_2 gas-molecular laser excited by high voltage direct current with maximum power of 10 watts at a wavelength of 10600 nm. The laser was mounted above the mass spectrometer and an optical system of mirrors and lenses which directed and focused the laser beam to impinge on the sample mounted directly below the ion source inside the time-of-flight mass spectrometer. The laser beam controlled by a solenoid actuated shutter provided pulses from 0.01 sec. to 1 sec. whereas operation with the open shutter permitted continuous heating of the sample. Accurate timing of pulse duration was accomplished with a fast response photo-diode used to trigger the oscillograph recorder timing galvanometer.

Various experiments in the continuous and pulsed mode of operation were undertaken to explore the utility of this experimental technique. Polystyrene, polyethylene and three methacrylate polymers, polymethylmethacrylate PMMA, polyethylmethacrylate PEMA, and polybutylmethacrylate

PBMA were continuously irradiated at an attenuated laser power of 0.4 to 0.7 watts at mass spectrometer ionization energy of 100 ev. The results of these studies show close agreement with the results of high temperature degradation studies using conventional electric furnaces.

The analog output system of the time-of-flight instrument permitted the time-resolved study of selected degradation products. In the pulsed mode of operation, laser power was varied from 3.5 to 7.9 watts with pulse durations from 0.05 to 1.03 sec. Pulsed laser degradation studies of polystyrene show a temperature dependency on the formation of degradation products. This temperature relationship shows increased products fragmentation at increasingly higher temperature evidenced by low molecular weight fragments.

CONTENTS

LIST OF FIGURES

LIST OF TABLES

Appendix

ABBREVIATIONS AND SYMBOLS

1.	cm	centimeter
2.	cw	continuous wave
3.	D C	direct current
4.	ev	electron volt
5.	gm	gram
6.	hr	hour
7.	in	inch
8.	IR	infrared
9.	kHz	kilohertz
10.	kv	kilovolt
11.	ma	milliampere
12.	m/e	mass to charge ratio
13.	mg	milligram
14.	min	minute
15.	mm	millimeter
16.	msec	millisecond
17.	nm	nanometer
18.	nsec	nanosecond
19.	sec	second
20.	V	volt

INTRODUCTION

Extensive studies of thermal degradation of organic polymers over the past few decades exist in the chemical literature. Many different experimental techniques have been employed to heat samples and to analyze the degradation products. These include mass spectrometry, infra-red spectrometry, ultraviolet spectrophotometry and gas chromatography.[1] Methods used to pyrolyze samples also are numerous, probably because such devices are relatively simple to construct and workers have designed units to fit their own specialized requirements. Levy[1] classified all pyrolysis methods into two major groups, those which degrade with pulsed energy and those which degrade with a continuous source of energy. Pulsed methods include resistive heating, high frequency induction, arc, and flash photolysis. Resistive electrical heating is widely used for continuous isothermal pyrolysis. This method utilizes a small furnace termed a microreactor. The small solid sample (10-50 mg) is rapidly inserted into the furnace where it is pyrolyzed. Although the actual temperature of the sample surface is difficult to determine, the maximum temperature of the pyrolysis products can be measured with a fast response thermocouple. Pyrolysis may occur at undetermined temperatures lower than measured in the microreactor.

Conventional furnaces limit pyrolysis to temperatures of 500-600°C. This results from the difficulty of retaining the sample at an elevated temperature for the time period required to characterize the degradation products. Polymers of high thermal stability, such as tetrafluoroethylene,

show a rate of weight loss at 500°C of only one percent per minute[2]. Degradation processes are typically first order and pyrolysis rate doubles for every 10°C rise in temperature. Consequently, the rate at 800°C would be very high. Actually, the measured rates are much lower than predicted because the thermal degradation of most polymers, including tetrafluoroethylene, is an endothermic process and low rates of heat transfer retard the degradation step. Despite these limitations, measured decomposition rates at temperatures in excess of 500°C are generally fast. It is difficult, using resistive heating methods, to obtain rapid thermal rise times. For example, at 800°C, a large portion of the sample will degrade and vaporize prior to reaching the temperature range of interest. Madorsky[3] has observed that "All these problems could be minimized to some extent if the crucible holding the sample were heated by focusing on it some radiant energy and if automatic, rapidly recording instruments were used for measuring temperatures and loss of weight as functions of time." Since this "request" in 1963 and the development of the laser, studies of the vaporization of solid materials by focused laser radiation have been carried out by a number of investigators. Although individual experiments characterized only a specific part of this process, a fairly complete quantitative understanding of this phenomenon, particularly for graphite and metals, has been obtained[4,5,6,7,8,9]. These studies utilized pulsed laser radiation, primarily ruby, and Nd-glass of wavelength 694.3 nm and 1060 nm respectively. Lasers operating in the normal pulsed mode or in the Q-switched pulsed mode have pulse durations varying from 1 msec. to 50 nsec. with

energies between one to five joules per pulse. These high power pulses mask much of the chemistry of the degradation process particularly in the degradation of organic polymers. High power deposition results in fragments rich in two and three carbon molecules[10, 11]. These severe degradation conditions have destroyed intermediate molecular weight fragments necessary to characterize molecular structure and degradation processes. Considerable information should be obtained by using lower power irradiations. This is theoretically feasible with pulsed lasers since the intensity of the laser beam is variable. However, sufficient power must be emitted during a single pulse to cause degradation; moreover, the surface temperature of the material may oscillate with the pulse cycle. Consequently, a low power continuous wave (cw) laser capable of providing the required energy flux may find more utility. Until the relatively recent development of the CO_2 molecular laser, wavelength 10600 nm. cw atomic-gas lasers have not been suitable for pyrolysis studies due to limited power (10 to 30 mw). Moreover, atomic-gas lasers operating in the IR region produce only a few milliwatts of power[12]. CO_2 lasers with maximum power from 10 to 150 watts can be obtained commercially. This is sufficient to pyrolyze most materials of interest.

The time-of-flight mass spectrometer is well suited for the study of fast reactions due to its ability to present ten or twenty thousand mass spectra per second. Time-of-flight spectroscopy remains one of the few mass spectrometric techniques which permit data to be taken over the entire mass range within the duration of a single laser pulse. Degradation products formed at the sample surface from a laser pulse lasting only a

few nanoseconds can be adequately analyzed by the time-of-flight mass spectrometer. Work with the pulsed laser time-of-flight mass spectrometer has been reported by Lincoln[10,13], Vastola[14,15], Knox[16,17], and Bernal[18]. These studies report degradation with both normal and Q-switched ruby and Nd-glass lasers using pulse times varying between 50 nsec. and 1 msec. and pulse energies of one to five joules. These studies indicate laser heating is a reliable method of obtaining simple mass spectra of solid materials such as polymers. However, the high energy and short time scale of the pulsed thermal event used in these studies limits investigation of the chemistry of degradation processes.

Polyethylene and a series of methacrylate polymers were chosen for study because they represent two extremes regarding pyrolysis products. Methacrylate polymers pyrolyzed in vacuum at temperatures from 150-500°C yield almost 100% monomer while in the case of polyethylene, pyrolysis under similar conditions yields hydrocarbon fragments varying in molecular weight from 16 (CH_4) to about 1000. Polystyrene was chosen as an intermediate between polyethylene and the methacrylate polymers because on pyrolysis in vacuum this polymer yields about 60% monomer.

Mass spectra have been obtained for polystyrene, polyethylene, polymethylmethacrylate PMMA, polyethylmethacrylate PEMA and polybutylmethacrylate PBMA under continuous heating by a cw CO_2 laser. By means of a mechanical shutter, the laser was operated in a pulse mode for time resolved degradation studies of polystyrene.

EXPERIMENTAL

1. Equipment

Time-of-Flight Mass Spectrometer

This study used a Bendix model 12-101 time-of-flight mass spectrometer equipped with a model S-14-107 ion source and M105-G-6 multiplier. The analog output system provides for electrometers which allow continuous monitoring of up to four individual mass spectra or m/e. All spectra were obtained with the repetition rate of 10 kHz. Accessory equipment included a Tektronix model 545A oscilloscope with a model C-12 oscilloscope camera. A Honeywell Visocorder model 906C oscillograph recorded the mass spectra. For readers not acquainted with the time-of-flight mass spectrometer a brief description of the operating principles follows: the mass spectrometer operates on the time-of-flight principle in which a group of ions in close physical proximity is given an impulse of kinetic energy directing them into a field-free drift tube toward a collector. All ions receive an equal energy impulse; their respective velocities vary according to their mass-to-charge ratios. Ions leave the accelerating region simultaneously and are allowed to drift a fixed distance prior to striking the collector. During the flight down the field-free drift tube the various ions separate based on their velocities which are inversely proportional to the square roots of the respective mass-to-charge ratios. As each group strikes the collector cathode the ions cause the release of secondary electrons which are focused by electric and magnetic fields along the electron multiplier. The electron pulses are amplified and detected by an oscilloscope. The lighter masses appear on the left of

the screen and heavier on the right. In addition to the oscilloscope anode the electron multiplier is equipped to selectively monitor individual mass spectra or m/e. The instrument is capable of monitoring a single m/e channel as a function of time with 0.1 msec. resolution.

The laser plume is ionized by bombardment with a pulsed electron beam in the ion source. This region is bounded by the backing plate and ion focus grid. The focus grid receives a negative pulse immediately after the electron beam is turned off. The attraction of the negative grid ejects all positive ions from the ionization region into the accelerating region. The front accelerating grid maintained at -2.8 kv imparts equal energy to the ions as they enter the drift tube. A schematic of the time-of-flight mass spectrometer is shown in Figures 1 and 3.

A standard vacuum pump and a mercury diffusion pump maintained normal operating pressure at 1×10^{-6} Torr. The vacuum pump was capable of attaining a pressure of 1×10^{-3} Torr in five minutes. These pressures were measured by an ionization gauge located 45 cm from the ion source and may not represent the actual pressure within the ion source. However, the operating pressure should be approximated by these values.

The instrument is capable of detecting ions with m/e ranging from 4 to 800. The flight time for an ion of m/e = 800 is well within a single cycle of the instrument operating at a repetition rate of 10^4 Hz. However, based upon the definition of resolving power used in this study the resolution of the instrument is limited to about 240. The ratios of $M/\Delta M$ define mass spectrometer resolution with the specification that the two ion beams, of equal intensity, M and $M + \Delta M$ can be recorded as two

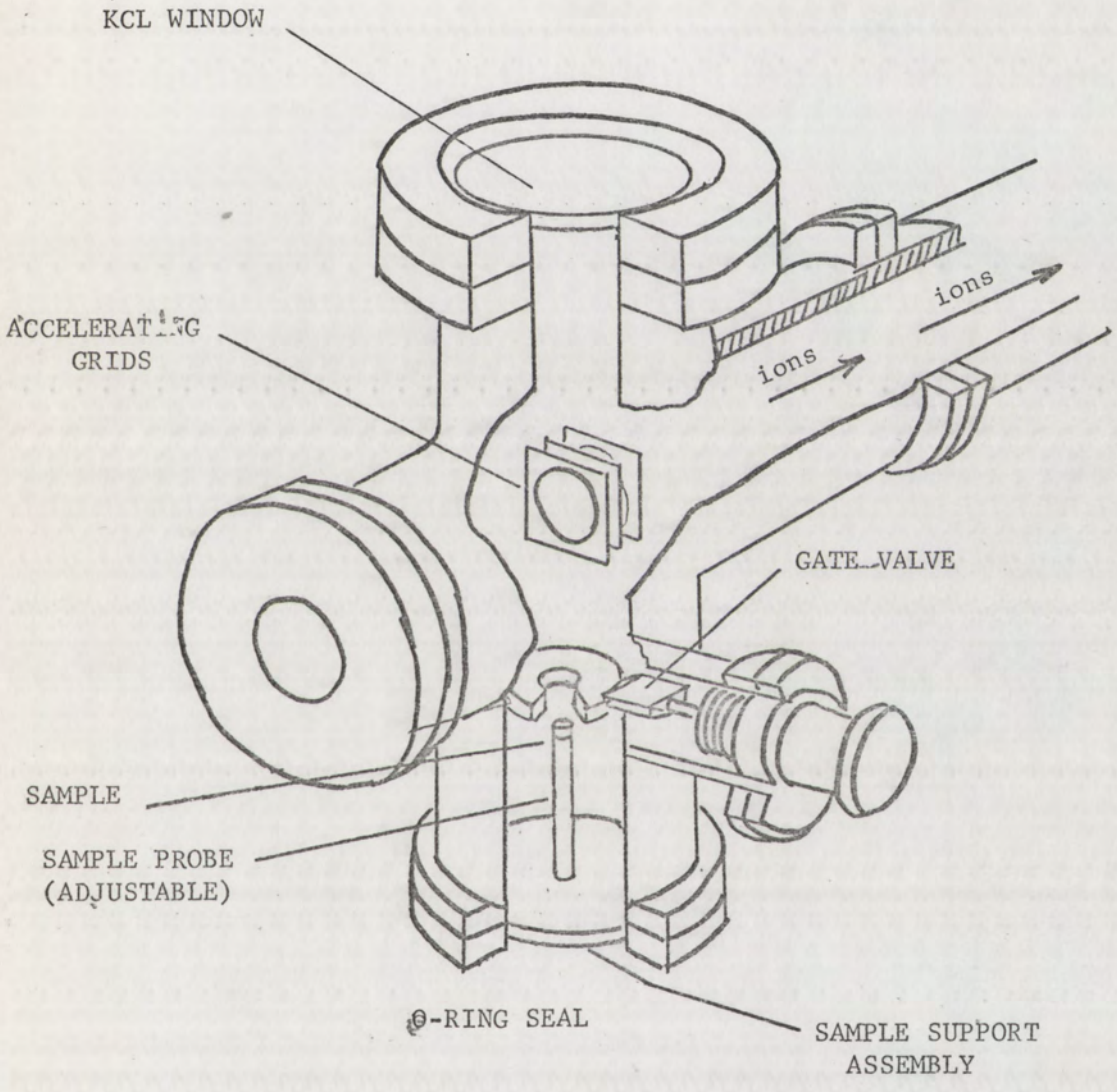

FIGURE 1. MASS SPECTROMETER GATE VALVE AND SAMPLE SUPPORT ASSEMBLY

peaks between which the recorder trace returns to less than 50% of the intensity of peak M. This definition is in common use[19]. The value of 50% allowed adequate distinction of mass peaks up to m/e = 240.

A gate valve assembly and vacuum tight sample support assembly, shown in figure 1, facilitated placing solid samples into the mass spectrometer without breaking vacuum. A stainless steel cylinder welded to the bottom blank-off header with guide rails attached to the cylinder top aligned and centered the gate valve over the sample inlet hole. A clamping mechanism forced the gate valve O-ring firmly in place over the periphery of the sample hole and the vacuum seal sustained pressures of 1×10^{-6} Torr.

CO_2 Laser

This study used a continuous flow CO_2 gas-molecular laser excited by high voltage direct current. The operational laser consists of four basic components: (1) laser cavity and optics, (2) gas metering and pumping system, (3) laser cavity cooling system and (4) high voltage DC power. A diagram of the CO_2 laser is shown in Figure 2.

A pyrex tube 4 cm. in diameter and 122 cm. in length formed the laser cavity. An annular pyrex glass cooling jacket enclosed the cavity tube. KCl windows mounted at a polarizing angle of $56^{\circ}8'$ terminated the laser cavity. The polarizing angle is defined as that angle of incidence for which the reflected polarized ray is at right angles to the refracted ray. Brewster's Law states "the tangent of the polarizing angle for a substance is equal to the index of refraction[20]." With n, the index of refraction and θ the polarizing angle then: $n = \tan \theta$. For n = 1.490,

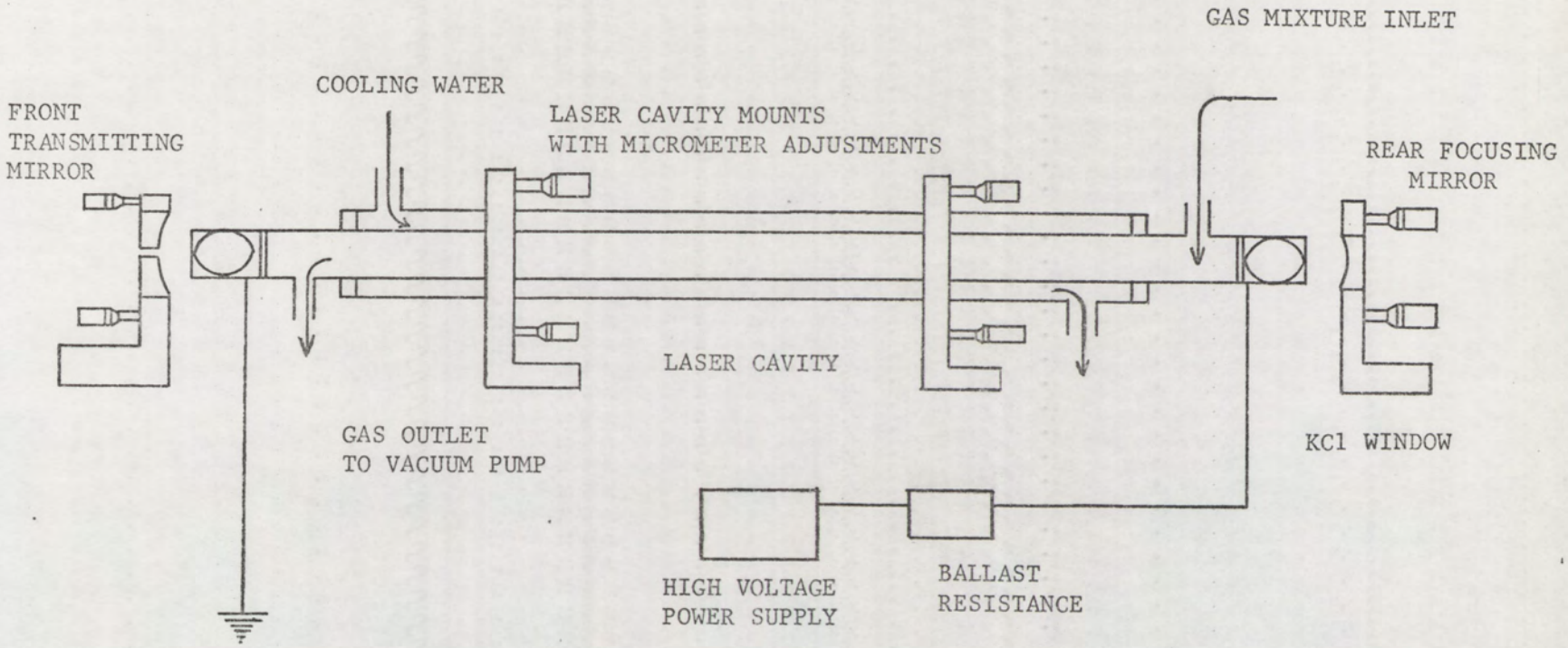

Figure 2. Diagram of CO_2 laser.

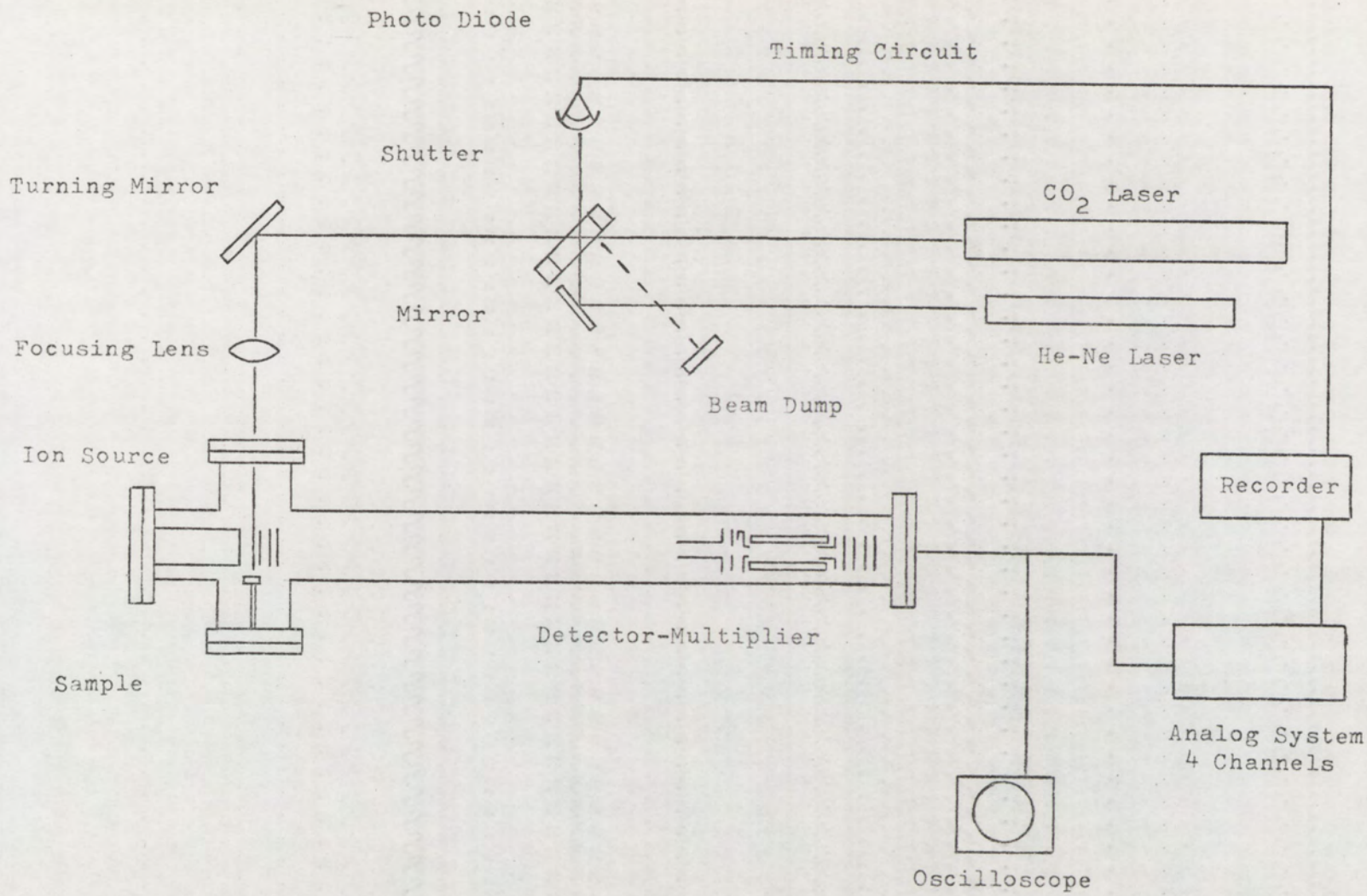

Figure 3 Laser-Mass Spectrometer System

the refractive index of KCl, $\theta = 56^{o}8'$. The gold-coated germanium terminal reflecting mirror was 2.25 inches in diameter with a focal length of one meter. The front transmitting mirror was 2.25 inches in diameter also made of gold-coated germanium. The mirrors were mounted in Lansing Optical Mounts with micrometer adjustments for the X and Y axes. An aluminum I beam served as an optical bench for attachment of the laser cavity-water jacket assembly. The mounting clamps, with micrometer adjustments for the X and Y axes, attached the laser cavity assembly to the optical bench. The mirror mounts similarly attached to the optical bench were not in direct contact with the lasing cavity. The means to separately adjust the alignment of both the laser cavity and the terminal mirrors greatly reduced the difficulty and time involved to get the system to lase and adjust for maximum power.

A Welch Duo-Seal model 1397 vacuum pump rated at 500 liters/min. maintained gas flow through the laser cavity. The gas inlet and outlet port located immediately behind the KCl windows of the laser cavity created an effective lasing cavity of about 1 meter. The gas mixture consisted of helium, nitrogen, and carbon dioxide controlled by a flow meter for each gas. The standard commercially available gases combined in the manifold and mixed before entering the laser cavity. Helium, nitrogen and carbon dioxide flow rates were respectively 10, 7, and 5 $ft.^{3}/hr.$ at a pressure of 20 Torr. A Veeco thermocouple gauge located downstream from the laser cavity monitored the pressure.

A submersible pump in a five gallon reservoir maintained at room temperature provided rapid flow of coolant water through the annular

water jacket. This cooling arrangement allowed the laser tube temperature to rise only about $10^{o}C$ after 30 minutes of continuous laser operation. A chilled water cooling system would be more desireable because the laser would be more stable, and powerful.

A Del Electronics Corporation model PSC 20-150 power supply provided the high voltage direct current. The power supply rated a maximum of 20 kv and 150 ma. The ballast resistance consisted of ten, 50,000 ohm, 200 watt resistors connected in series for a total resistance of 500,000 ohms. The ballast resistance was in series with the high voltage power supply and the laser cavity. The high voltage lead to the terminal end of the laser cavity terminated with a ground lead from the transmitting end of the laser cavity. The sharp ends formed by the Brewster angles were conducive to high voltage arcing from the laser cavity to the mirror mounts at ground potential. The use of high voltage putty on the discharge points alleviated this potentially dangerous condition.

A helium-neon laser was used to align the laser cavity with the terminal mirrors. Removal of the front transmitting mirror of the CO_2 laser from its mount allowed the He-Ne laser beam to pass through the laser cavity and reflect off the rear focusing mirror. Initial alignment was achieved when the reflected He-Ne beam coincided upon itself.

Laser Characterization

A Coherent Radiation Laboratory model 201 thermopile monitored total continuous power of the laser. Maximum continuous power obtained was

10 watts at a wavelength of 10591.5 nm and a beam diameter of 0.5 cm. which correspond to a power density of 51 watts/cm^2. The stability of the laser power, monitored frequently over a period of three months, did not vary more than $\pm$ 0.2 watts from the desired power setting over the range from 1.5 to 10 watts. After periods of continuous laser operation from 15 minutes to 30 minutes the laser power varied less than $\pm$ 0.1 watt from the desired power.

Voltage and current calibration at laser power varying from 1.5 to 8 watts, shown in Table 1, reduced the necessity of measuring laser power after each adjustment of the power supply. Laser power observed before and after each period of use was very consistent with Table 1.

The working efficiency of the laser is defined as the ratio of the output power to the input power:

$$\text{Efficiency} = \frac{\text{OUTPUT POWER}}{\text{INPUT POWER}}$$

Where input power is calculated from:

$$P = I^2R$$

P = power in watts; I = current, R = resistance in ohms and the output power is that measured by the thermopile. A graph of laser efficiency versus power computed from Table 1 is shown in Figure 4.

Laser Beam Focus-Optical System

The CO_2 laser mounted horizontally above the mass spectrometer formed the laser-mass spectrometer system shown in Figure 3. A highly polished,

TABLE 1

Laser Power as a Function of Power Supply Current and Voltage

Laser Power (watts)	Current (ma)	Voltage (kv)
1.5	3.0	12.6
2.0	3.5	12.8
2.5	4.5	13.2
3.0	4.75	13.4
3.5	5.5	13.5
4.0	6.28	13.7
4.5	6.70	14.0
5.0	7.5	14.3
5.5	8.5	14.6
6.0	9.3	15.0
6.5	10.25	15.5
7.0	11.5	16.0
7.5	12.75	16.6
8.0	13.75	16.8

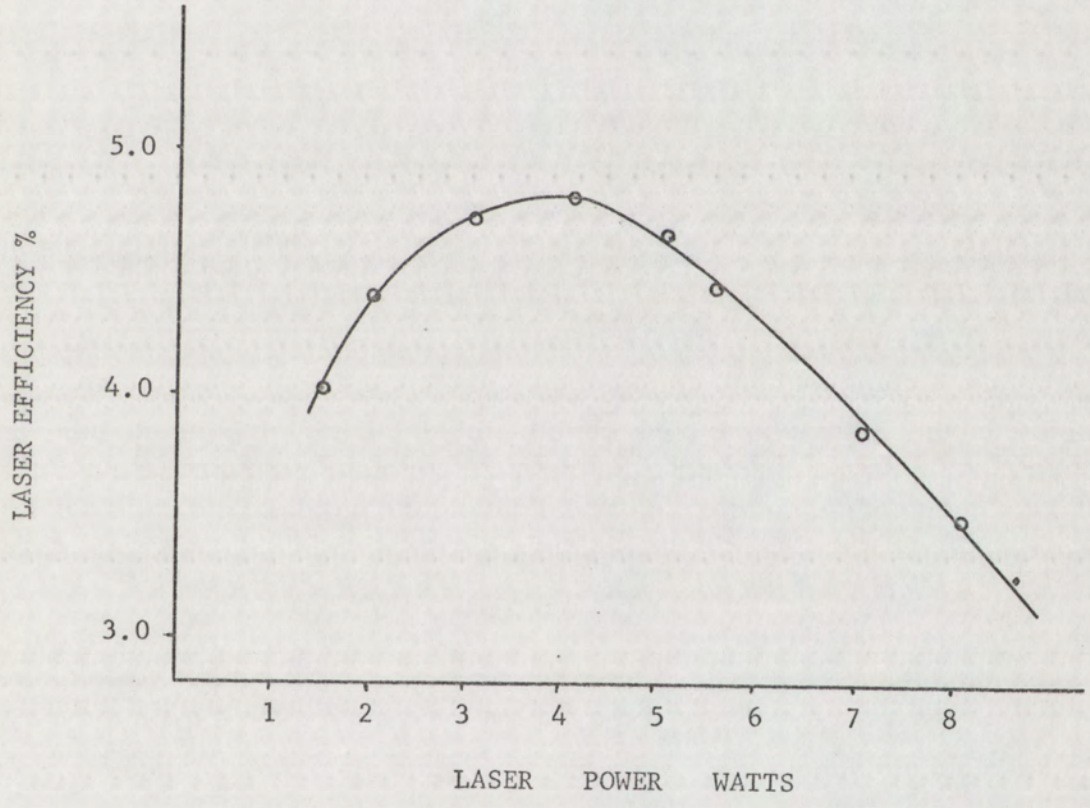

Figure 4. CO_2 laser efficiency.

high purity oxygen free, copper mirror directs the beam downward through a germanium lens, with a focal length of 25 cm. The beam enters the mass spectrometer through a KCl window mounted in the top blank-off header and passes between the backing plate and 1st grid on the ion source which are spaced 0.635 cm. apart. The focused beam impinges on the sample located 6 cm. below the ionization region of the ion source. Reflectivity of the copper mirror measured 98.4% of the aluminum standard on a Beckman IR-9 Spectrometer at a wavelength of 10600 nm. The copper mirror was polished with 240 grit, then 600 grit followed by 600-soft, abrasive papers and finished on a micron diamond buffing wheel.

Power loss through the focusing lens and KCl window was 9% of the incident beam; most of this loss being attributed to the KCl window.

Shutter-Timing System

A Beattie-Coleman oscilloscope camera shutter actuated by a solenoid from a remote control switch box regulated the beam for continuous and pulsed operation. The shutter speed varied from 10 milliseconds to 1 second or could be set in the time exposure position for continuous laser operation. The reproducibility of the camera shutter varied slightly upon occasion, however, the duration of the shuttered laser pulse was accurately determined by a marker system using a photodiode with extremely rapid response. As shown in Figure 3 a University Physics model PS-311 helium neon alignment laser activated the photo-diode (type 1N2175) when the camera shutter was open. The photo-diode, fully conductive in about 5 nano-seconds, allowed a 40 millivolt signal (provided

by a 1.5V D cell in series with a 2 megohm potentiometer) to be sensed by a miniature timing galvanometer in the oscillograph recorder. The duration of the laser pulse appeared as a rectangular pulse on the recording paper and the oscillograph internal timing marker allowed the duration of the laser pulse to be determined within 1 msec.

Theory of Operation

A comprehensive discussion of CO_2 laser theory and development is given by Patel[32]. The CO_2 laser derives its energy from transitions between the vibrational-rotational energy levels of the molecule. Quantum-mechanical selection rules require a change in the vibrational state of the molecule be accompanied by a change in the rotational state as well. Therefore, in the infra-red region of the spectrum there are vibration-rotation bands. Basically, the appearance of the band can be interpreted by adding the vibrational and rotational energies of the molecule. In the simplest case, selection rules allow only those transitions with a change in the rotational angular momentum equal to $\pm$ h/2π where h is Plancks constant. The resultant band has two branches, the P-branch which corresponds to +h/2 and the R-branch which corresponds to -h/2π. The carbon dioxide molecule is linear and symmetric and has 3N-5 = 4, where N = 3, degrees of vibrational freedom. They are symmetric stretch, asymmetric stretch and a degenerate pair of bending modes of vibration.

Excitation of the vibrational modes in the ground state CO_2 molecule can result from high voltage electric discharge. In such a discharge a large number of electrons collide with the CO_2 molecules and excite them

to various vibrational levels. The electrons preferentially excite the CO_2 molecules to a level corresponding to the asymmetric stretch mode of vibration. As shown in Figure 5, the asymmetric stretch mode corresponds to the upper laser level (001). Transitions from excited level (001) to low or excited level (100) result in the emission of photons with wavelength of 10591.5 nm.

Molecules that are excited beyond the (001) level may contribute to the laser action by undergoing a collision with a molecule in ground state (000). Vibrational energy transfer between unexcited molecules and molecules in excited states higher than the 001 level can take place resulting in a molecule in the upper laser level (001). These interactions are termed resonant in that there is a redistribution of the energy within the excited molecule with no loss of internal energy to thermal or kinetic energy.

The excited CO_2 molecule must decay to the ground state before the molecule can again lase. Upon emitting a laser photon of wavelength 10591.5 nm. the CO_2 molecule goes to the lower laser level (100). The molecules at the lower laser level decay to the (000) level through radiationless collisional energy transfer steps. The lower laser level has nearly twice the energy required to excite the ground state CO_2 molecule to the (010) level. Therefore, a resonant collision between a (100) level CO_2 molecule and a ground state CO_2 molecule may result in excitation of both molecules to the (010) level. The CO_2 molecules of the (010) level decay to the ground vibrational state by non-resonant collisions with other CO_2 molecules, other gases, or the walls of the

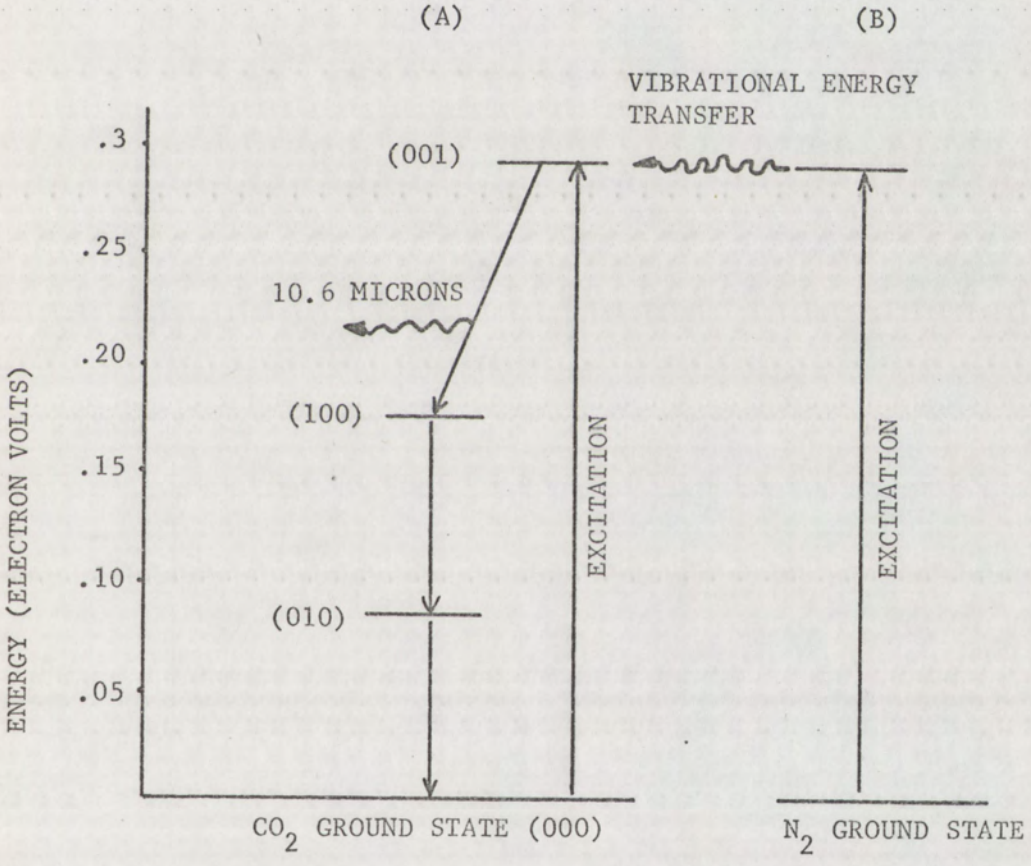

Figure 5. (A) Energy level diagram of low level vibrational states of CO_2.

(b) Selective excitation of CO_2 by N_2. Rotational levels have been excluded.

laser cavity.

Selective excitation of the ground state CO_2 molecules to the upper laser level occurs when nitrogen gas is added to the laser. The vibrational excitation energy of the N_2 molecule is nearly equal to that of the upper laser level (001) of the CO_2 molecule (see Figure 5). Therefore, upon the collision of an excited N_2 molecule and a ground state CO_2 molecule, vibrational energy is transferred resulting in an excited CO_2 molecule at the (001) level and a ground state N_2 molecule. In an electrical discharge at low pressure about 30% of the N_2 is excited to the (001) level. This resonant process of selective excitation of the CO_2 molecule to the upper laser by N_2 has been shown to be very efficient.[32]

Increased laser power and efficiency can be obtained by increasing the rate of decay from the (010) level to the ground state. This process takes place when kinetic energy is transferred during a collision with another body. The rate of this process depends on the nature of the other particle. At a pressure of 1 torr and 25°C carbon dioxide has about 100 de-esciting collisions per second and helium has about 4,000 such collisions per second. Therefore, helium gas is used in the CO_2 laser system.

Even though the (001) to (100) vibrational transitions contain a number of possible P-branch and R-branch transitions, laser emission can be made to occur on a single P-branch transition. Certain P-branch transitions show laser emission even when there is only partial inversion of the CO_2 population.[32] With complete CO_2 population conversion, both the P-branch and R-branch show laser emission but P-branch transitions

tend to show greatest intensity. The rotational transition with the highest intensity will start oscillating first. This will be the strongest P-branch transition. The competition among possible laser transition results in one P-branch dominating. By using a grating or prism to prevent oscillation of the stronger P-branch transition, laser action is possible on the weaker P-branch or R-branch transitions. Such mechanisms indicate the possibility for a tunable infrared laser.

Laser action by itself is not very practical, therefore linear laser cavities and focusing mirrors are used to form the laser photons into a useful beam. The front mirror, termed the transmitting mirror, has a small non-reflective center. After several reflections between the focusing mirrors, the photons converge and the resultant beam exits the cavity through the "window" in the front mirror. Mirrors and lenses can then be used to manipulate the beam however desired.

2. OPERATIONAL TECHNIQUES

Interpretation of Mass Spectra

Interpretation of mass spectra in this study was somewhat simplified by the known composition of the sample and by prior identification of the degradation products. The basic problem was therefore one conforming the m/e of any mass peak.

The residual air present in the instrument provided a convenient background spectrum of mass markers at m/e = 14, (N^+ or N_2^{++}), 16 (O^+ or O_2^{++}), 18 (H_2O^+), 28 (N_2^+), 32 (O_2^+) and 40 (Ar^+) as shown in Figure 6. Mercury vapor from the mercury diffusion provided very convenient

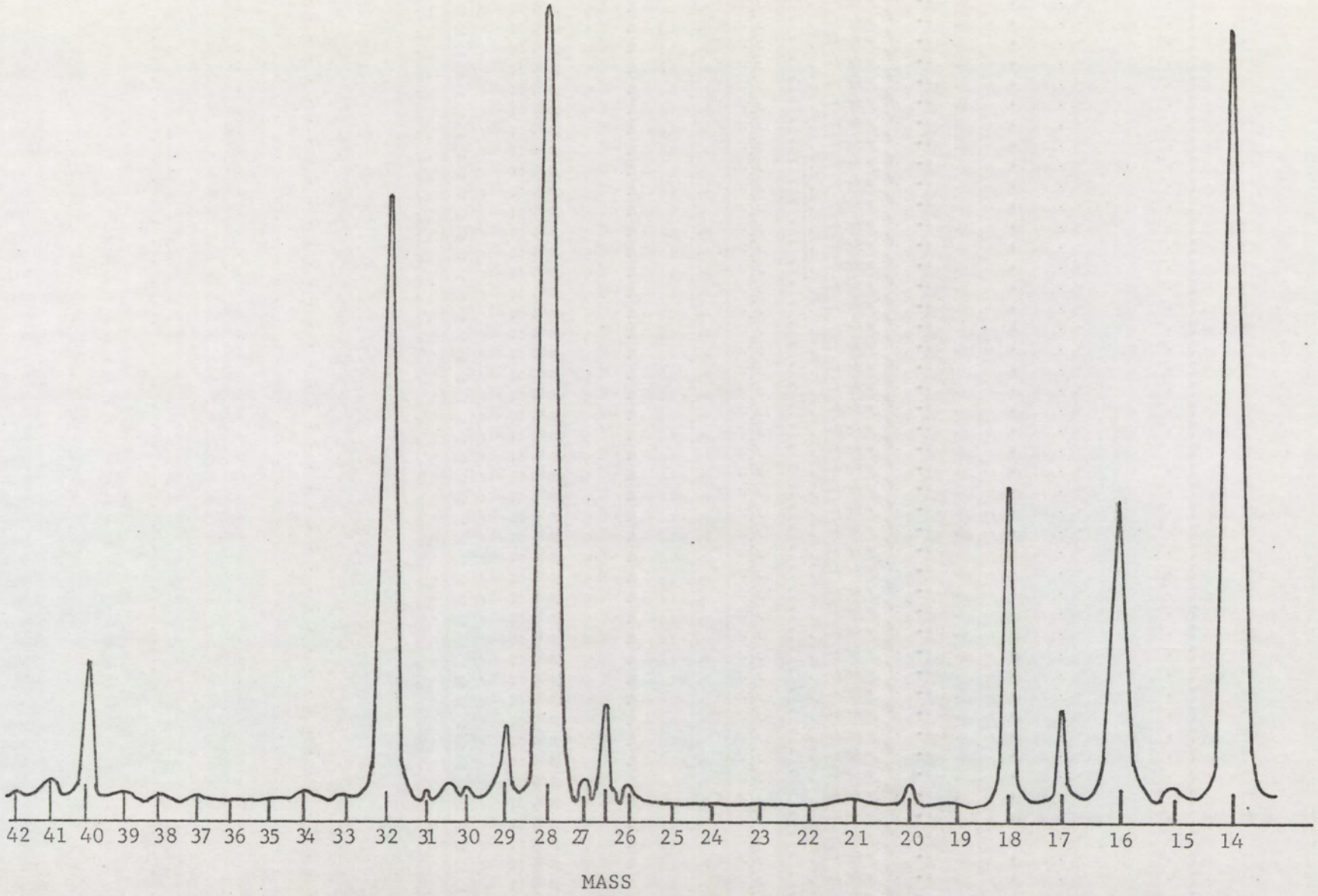

Figure 6. Background spectrum of air. Spacing of perfect square mass peaks 121 divisions based on a scale of 40 divisions per inch.

mass markers at m/e = 196, 198, 199, 200, 201, 202, and 204. The doubly charged, more abundant mercury isotopes of mass 200 and 202 also appear on the spectrum at m/e = 100 and 101. This collection of "built in" mass markers was extremely helpful for quick identification of adjacent mass peaks, however, in other instances the background spectrum masked the presence of sample mass peaks. In addition to the mass markers inherent to the mass spectrometer, perfluorokerosene and sulfur hexafluoride were used. The SF_6 was most useful because it gave a spectrum with mass peaks at 146, 127, 89, 70, and 51 which correspond to the loss of a fluorine atom of mass 19.

The spectrum of many polymeric materials gives rise to mass peaks from m/e = 14 through 110. In such cases the mass peaks are identified by simply counting from mass markers. In many instances however, there are gaps between mass peaks and these gaps make it necessary to interpolate the mass spacings. A simple method of calculating the position of mass peaks was developed to complete the gaps between existing mass peaks and verify their mass numbers. The distance from a known perfect square mass peak to an unknown mass peak can be determined with the following equation:

$$\left| A - B \right| X \quad S \quad = \quad D \qquad (2)$$

where A is a mass peak with a perfect square m/e, B is the mass peak whose position is to be determined, S is the spacing between mass peak of perfect square m/e in arbitrary units, D is the distance from the known mass peak A to unknown mass peak B in same units as S. As shown in Figure 6, the spacing between m/e = 16 and 25 is 121 divisions on a scale of 40

divisions per inch. Applying equation (2) with A = 36, B = 40 and S = 121 the position of mass peak 40 is shown to lie about 1 inch (39 divisions) above the position for mass peak 36.

From a combination of various methods of interpolation and identification of mass peaks it was possible to make a mass ruler which covered the mass range from 12 to 204. Slight daily variations in the electronic stability of the instrument limited accuracy of the mass ruler and made it unreliable for determining spectra within one mass unit.

Equipment Maintenance

Normal mass spectrometer maintenance is thoroughly covered in operation manuals and textbooks, however, the operating conditions of this study required additional procedures to keep the instrument operable. The close proximity of the sample to the ion source increased the spattering and deposition of polymer vapor on the ion source and accelerating grids, leading to an impairment of the quality of spectrum obtained or malfunction of the instrument.

After periods of 45 minutes to 1 hour of continuous or pulsed operation the ion source was removed from the mass spectrometer, disassembled and cleaned. All parts were immersed in acetone after light scrubbing with a cotton swab, and placed in an ultrasonic cleaning bath for two hours. After removal from the bath the parts were rinsed in ethyl alcohol and allowed to air dry. The ion source housing was scrubbed in ethyl alcohol and allowed to air dry. Careful and frequent cleaning of the accelerating grids appeared to extend their operational life by a factor of ten. Without cleaning, the grids failed in about 4 hours of operation

under these severe conditions.

The inside walls of the mass spectrometer were cleaned with alcohol at less frequent intervals in order to reduce the background spectrum from outgasing polymer vapor condensed on the spectrometer walls.

Laser maintenance primarily involved periodic polishing of the KCl windows to prevent unnecessary power loss. As the KCl windows adsorbed water from the air the surface became slightly cloudy resulting in loss of laser power. In some instances the high voltage discharge in the laser cavity appeared to cause small pits in the surface of the windows. This pitting resulted in loss of effective laser power by dispersion of the beam.

The salt windows were restored to the desired optical transmission characteristics by polishing with 420 grit paper to remove pitting followed in succession by 600 grit and 600-soft metallurgical polishing paper. Final polishing on 5 and 1 micron diamond buffing wheels was performed every six weeks.

A plexiglass box mounted over the mass spectrometer along the laser beam path provided a safety shield to protect against accidental reflection of the beam. Even though the infrared radiation of the laser beam is not visible, the greater danger in operating the laser is high voltage discharge which can result in cardiac arrest and seizure of the respiratory muscles.

3. CONTINUOUS IRRADIATION STUDIES

Experimental Conditions

For continuous irradiation of polymers, the sample was cut to a

diameter of 0.75 cm. and placed on the sample probe inside the mass spectrometer. Pinholes, 1 mm and 2 mm in diameter, attenuated the laser beam to avoid saturating the ion source and detector. The pinholes were drilled in a 1/8 inch thick asbestos disk and positioned on the top blank-off header. Attenuated laser power through the 1 mm, 2 mm, and 3 mm diameter pinholes measured within the mass spectrometer by the thermopile is shown in Figure 7. Reduction of laser power limited deposition of sample vapors on the accelerating grid and maintained their operational life.

Adjustment of laser power presented a stable, well defined oscilloscope display of the mass spectrum and maintained a pressure in the mass spectrometer of 1×10^{-5} Torr. The scan rate with the best resolution for the least time, covered the mass range from m/e = 4 to m/e = 210 in about 1.5 minutes.

For most continuous and pulsed studies the mass spectrometer operated in the pulsed positive ion mode with ionization energy of 100 ev, filament current 2.5 amperes and detector sensitivity of 100 nanoamperes.

Polystyrene

This experimental investigation used CADCO polystyrene No. 7 obtained from Cadillac Plastic and Chemical Company, Detroit, Michigan. The manufacturer specifies the polymer to be of high purity with molecular weight of 230,000 and a density of 1.046 gm/cm^3.

A polystyrene sample was irradiated in the mass spectrometer to study the effects of ionization energy on product fragmentation at energies of 30 ev, 60 ev, 70 ev, and 100 ev. Laser power was 7 watts attenuated by

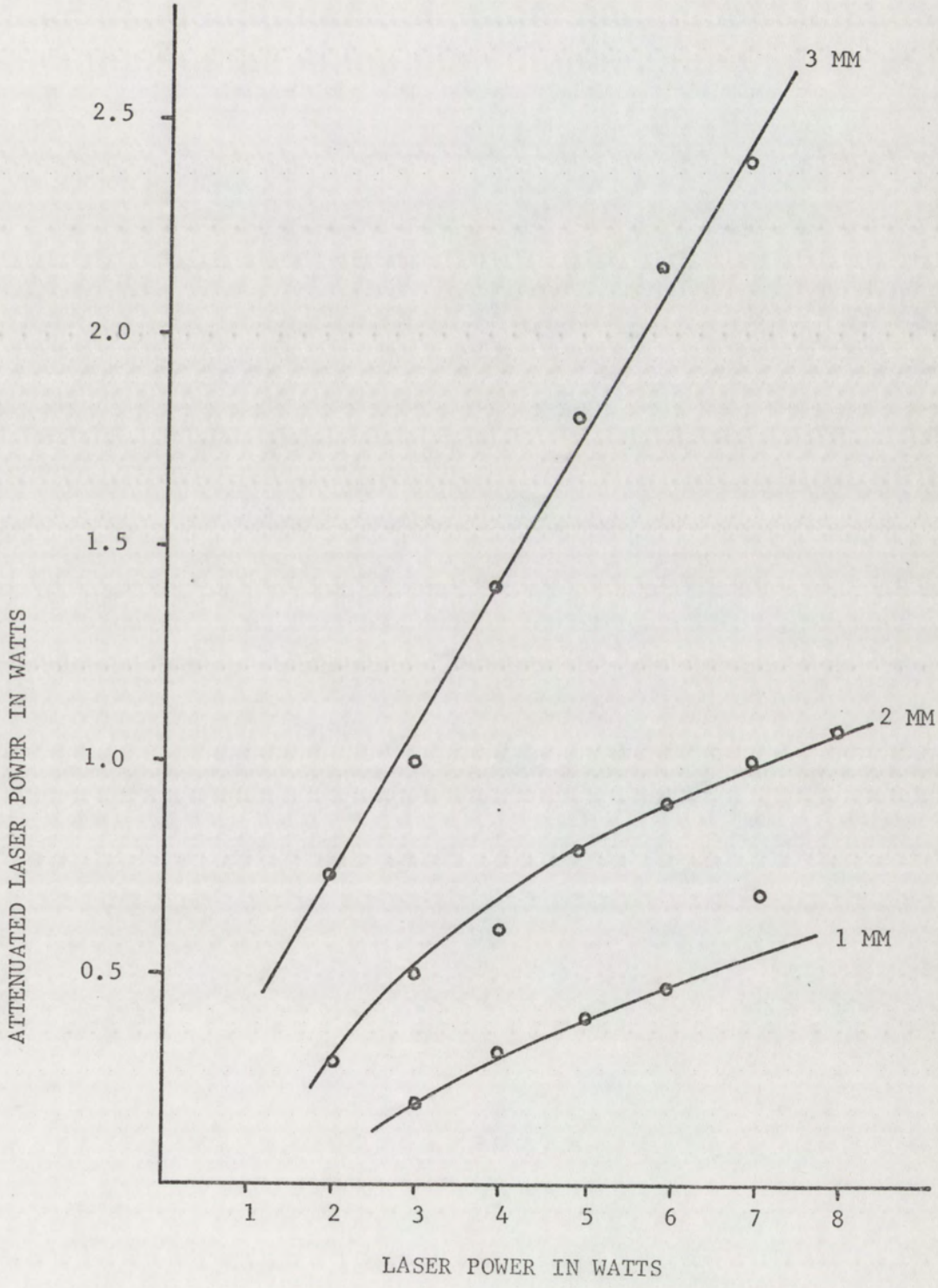

Figure 7. Laser power attenuated by 1 mm, 2 mm and 3 mm diameter pinholes.

1 mm pinhole to an incident power of 0.5 watts. The same sample exposed at the four ionization energy levels cooled for about 10 minutes between each irradiation.

The spectral range from m/e = 196 to 400 was scanned to detect the dimer and trimer of polystyrene. The laser power was 5 watts attenuated to an incident power of 0.4 watt. The mass spectrometer ionization energy was 100 ev with maximum electrometer sensitivity of 0.01 nanoampere.

Polystyrene irradiated in the presence of oxygen characterized the effects of a reactive atmosphere on degradation products. A Bendix Gas Sample Inlet accessory provided a steady and continuous gas flow directly into the ion source of the mass spectrometer through the gas inlet valve. The operating pressure was 5×10^{-6} Torr measured by the ionization gage. The sample was irradiated at a laser power of 3 watts attenuated by a 3 mm. pinhole to an incident power of 1 watt with mass spectrometer ionization energy 100 ev and detector sensitivity of 100 nanoamperes.

An effort to observe the effects of an inert atmosphere on degradation products was conducted under the same experimental conditions previously described for degradation in the presence of oxygen. This experiment used nitrogen gas in place of oxygen.

Polyethylene

E. I. DuPont de Nemours and Company supplied the polyethylene samples composed of very long, nearly branch free carbon chains with a density of $0.967\ g/cm^3$.

Polyethylene samples were placed in the mass spectrometer for continuous

laser decomposition at a laser power of 6 watts attenuated with a 2 mm pinhole to an incident power of 0.9 watt. The mass spectrometer ionization energy was 100 ev and the detector sensitivity was 10 nanoamperes.

Methacrylate Polymers

Three methacrylate polymers studied under continuous laser irradiation were polymethylmethacrylate PMMA, polyethylmethacrylate PEMA, and polybutylmethacrylate PBMA, products of the Rohm and Haas Company.

All samples were exposed to a laser power of 4.5 watts attenuated to an incident power of 0.6 watts. Mass spectrometer ionization energy was 100 ev and detector sensitivity was 10 nanoamperes. Comparison with background scans made prior to the irradiation of each sample determined principal product mass peaks. The background spectrum mass peaks were deleted from polymer spectrum except in those instances where a background mass peak appeared to be enhanced by a degradation fragment.

4. PULSED IRRADIATION STUDIES

Experimental Conditions

Pulsed studies of polymers used the analog output system to simultaneously monitor three mass peaks. As the sample was being continuously pyrolyzed, the gate marker of each of the three monitoring electrometers was set using the oscilloscope display to position the gate marker directly on the desired mass peak. Mass peaks seen on the oscilloscope were identified from a previously recorded sprectrum of the sample. The 50 nanosecond gate width of the monitoring electrometer assured no interference

from adjacent peaks. Precise centering of the gate marker was ascertained by adjusting for maximum deflection of the recorder galvanometer measuring the ion current for that mass peak.

With the mass spectrometer-analog system set to record the event, the camera shutter was set for the desired pulse duration and remotely triggered. For most pulsed studies recorder chart speed was 2.5 in/sec. To conserve recorder paper, the chart-drive switch was also remotely controlled by the same switch used to trigger the camera shutter.

Polystyrene

Shuttered or "pulsed" laser beam studies of selected degradation products determined the kinetics of degradation processes and the effects of parameters such as electron ionization energy, laser power and pulse width.

An ionization efficiency curve for the monomer of polystyrene m/e = 104 and the benzene fragment m/e = 78 was determined at a laser power of 7.9 watts with constant pulse width of 0.65 seconds. The electrometers monitored the monomer and benzene fragments at maximum sensitivity of 0.01 nanoamperes. The electron ionization energy was increased 1 ev after each irradiation and the sample cooled for about 3 minutes between exposures. The intensity of each ion was determined by measuring the maximum amplitude of the recorder trace with a scale of 20 divisions per inch.

An experiment was undertaken to detect ions produced by CO_2 laser irradiation of polystyrene. The sample probe was adjusted placing the sample about 3 cm. below the center line of the ion source. The electron

gun filament current was switched off and the ionization voltage control was set at 0 ev. The electrometers were set at maximum sensitivity of 0.01 nanoampere to monitor the monomer, m/e = 1-4 and benzene m/e = 78. The laser was set for a maximum power of 8 watts and the sample was exposed to increasingly longer laser pulses beginning with a duration of 0.065 seconds.

Polystyrene monomer, the monomer derived benzene fragment and the ethylene fragment were selected for study of degradation kinetics. The recorder galvanometers, adjusted to establish a separate base line for each ion, facilitated interpretation of each recorder trace. The laser power varied between 3.5 and 7.9 watts and the spectrometer operated at an ionization energy of 100 ev and electrometer sensitivity was 100 nanoamperes.

RESULTS AND DISCUSSION

1. CONTINUOUS IRRADIATION STUDIES

Laser induced thermal decomposition leads to a greater molecular fragmentation than that found with electron bombardment even with electron energies of 70 ev or higher. For instance, pulsed ruby laser interactions with polystyrene have been shown to lead to a product distribution rich in low molecular weight gases, acetylene, ethylene[28]. In this work, both laser degradation and electron degradation effected the molecules under study. Laser degradation can be thought of as an intense, localized thermal interaction while electron bombardment is best visualized as an overlap of electric force fields and not a sudden collision that injects 70 ev or more into a specific molecule[37].

Polystyrene

Polystyrene was chosen for initial continuous studies since this compound has been investigated under several different thermal degradation techniques. Table 2 contains the results of laser irradiation with this material using an ionization energy of 30 ev, 60 ev, 70 ev, and 100 ev. If we assume that the laser-induced degradation process is not affected by ionization occurring in the ion source, the extent of fragmentation increases with increasing ionization energy, similar results are found in conventional mass spectrometric analyses. The principal fragments (m/e = 51, 77, 78, 91) reach relative maximum intensity at 60-70 ev and then decline at higher energies while the monomer fragment (m/e = 104) is fairly constant, relative to the m/e = 103 fragment, over the range of

TABLE 2

Analysis of Products from Laser Pyrolysis of Polystyrene at Ionization Energies of 30eV, 60eV, 70eV, and 100eV Relative Intensity as Percentage of Base Peak 104.

m/e	Rel. Int.			
	30eV	60eV	70eV	100eV
27	-	12	12.5	10.5
39	-	16	15	13
50	-	14.7	15	13
51	-	33.3	27.5	23.2
52	-	16	17.5	10.5
59	11.5	-	7.5	1.0
62	-	4	5.0	3.0
63	11.5	10.6	10	8.1
65	-	5.3	7.5	5.8
74	-	5.3	5.0	5.8
75	-	6.7	5.0	4.7
76	-	8.0	5.0	4.7
77	-	25.4	20	15.1
78	15.4	38.9	30	24.4
79	-	-	5.0	4.7
89	-	3.0	5.0	3.5
91	23	18.7	42.5	29
102	-	-	10	7.0
103	-	40	35	37.2
104	100	100	100	100

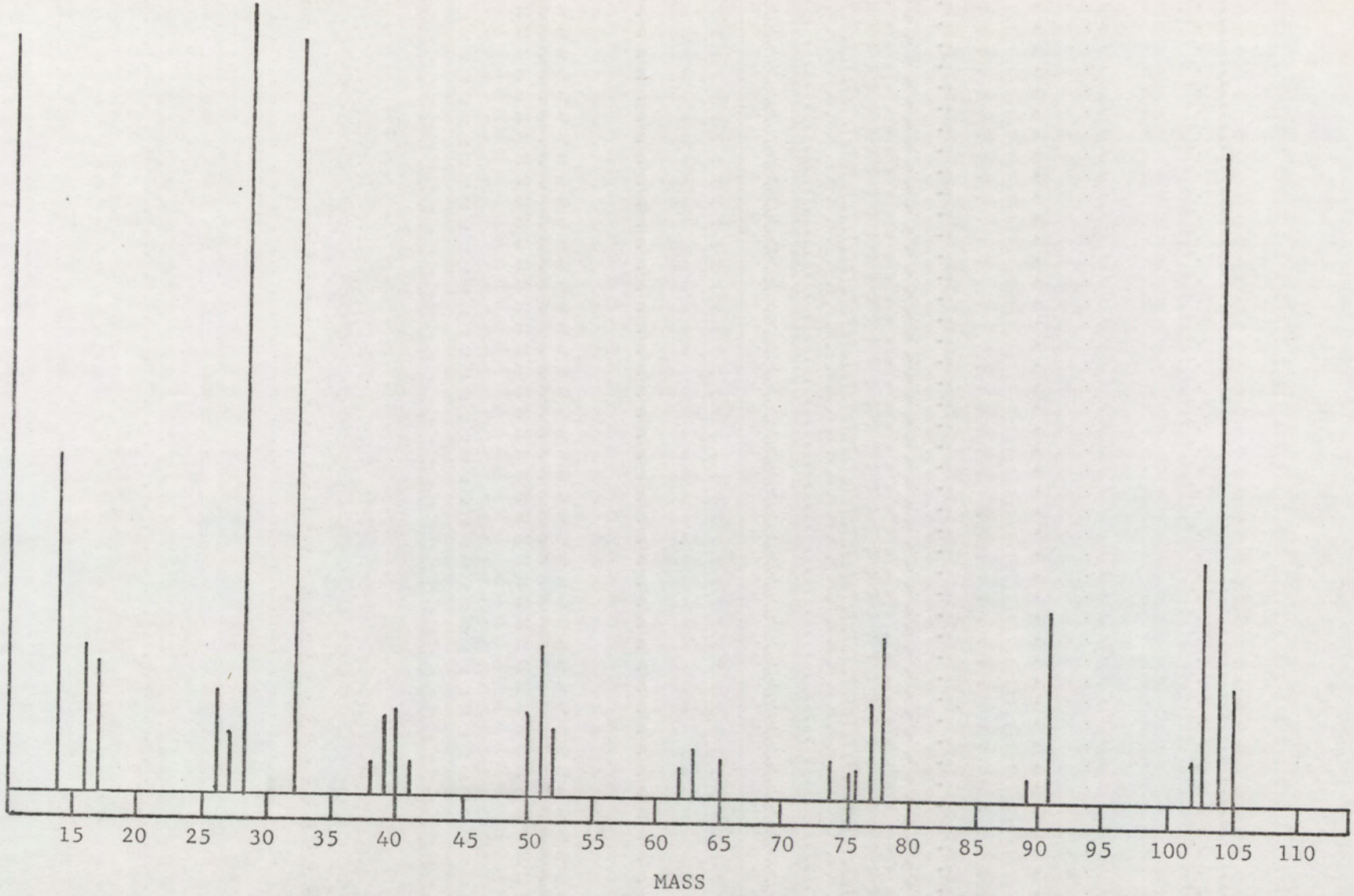

Figure 8. Mass spectrum of polystyrene obtained under continuous laser pyrolysis.

60-100 ev.

Reproducibility of results obtained from polystyrene at a laser power of 7 watts attenuated to an incident power of 0.5 watt with an ionization energy of 100 ev is shown in Table 3. Results indicate that the reproducibility approaches an average of $\pm$ 15 percent, typical of such mass spectral experiments.

The dimer (m/e = 220) and trimer (312) fragments as well as larger fragments located at m/e = 279 and m/e = 296 also appear in the spectra. Staudinger[22] suggested the following mechanism of chain scissions to account for the dimer and trimer degradation products

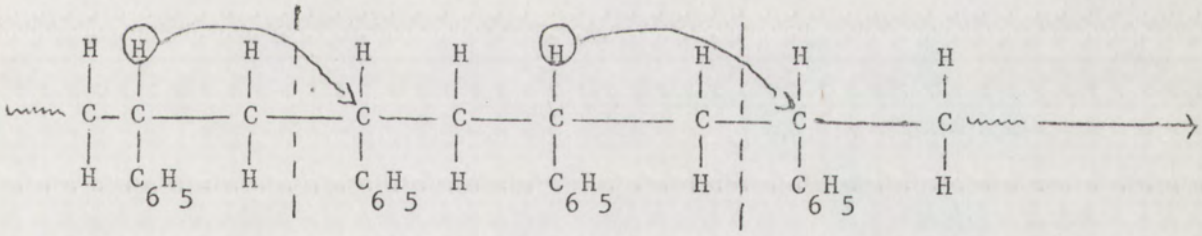

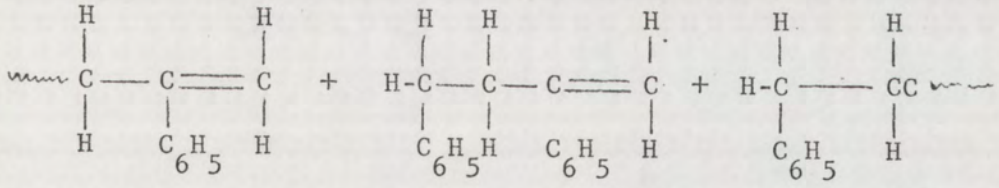

Degradation must begin by breaking either a C-H bond or a C-C bond. Evidence is that C-H bonds are weaker than C-C bonds. Also, bonds between hydrogen and the tertiary carbon atoms are weaker than those between hydrogen and a secondary carbon. Thus, initially, hydrogen is abstracted from the tertiary carbon and transfered to another tertiary site. On this basis, reasonable structures for the trimer m/e = 312 and

TABLE 3

Mass Spectral Analysis of Products from Laser Pyrolysis of Polystyrene in Vacuum, Ionization Energy 100 ev.

	Rel. Int.					
m/e	Expt.	1	2	3	4	Rel. Dev. %
27		6.5	10.5	12	12.5	18
39		11.1	12.8	16	15	13
50		15.6	12.8	14.7	15	6.2
51		29.2	23.2	33.3	27.5	10.6
52		13.6	10.5	16	17.5	16
62		4.5	3.5	4	5	11.6
63		7.2	8.1	10.6	10	15
65		3.9	5.8	5.3	7.5	17.9
74		7.8	5.8	5.3	5	18
75		5.8	4.7	6.7	5	12.7
76		5.8	4.7	8	5	19.6
77		19.5	15.1	25.4	20	13.5
78		35.7	24.4	38.9	30	15.5
79		4.5	4.7	*	*	2.2
89		2.6	3.5	2.7	5	23
91		19.5	29.0	18.7	42.5	30
102		7.8	7.0	*	10	14.4
103		39	37.2	40	35	4.5
104		100	100	100	100	0

*Not available.

the dimer m/e = 220 are:

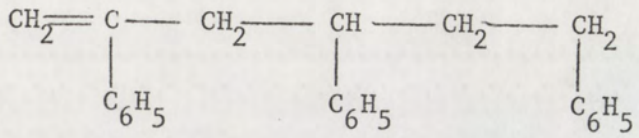

$C_{24}H_{24} = 312$

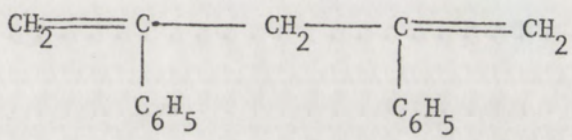

$C_{17}H_{16} = 220$

The smaller fragmentation products, m/e less than 104, are typical of those found in conventional mass spectral analyses of styrene[4]. These results therefore indicate laser induced thermal degradation at the sample surface predominately forms monomer with a small fraction of dimer and trimer. These species then undergo additional fragmentation in the ion source. The results of polystyrene degraded in the presence of oxygen are shown in Table 4. Jellinek[23] determined that oxidation of polystyrene occurs as follows:

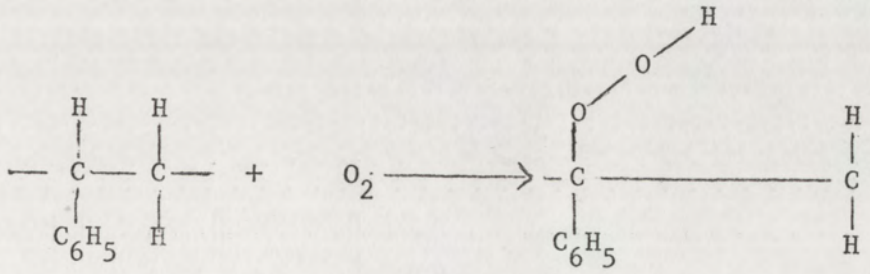

These hydroperoxide groups will then bring about chain scissions with the formation of keto and hydroxyl groups:

TABLE 4

Analysis of Products from Laser Pyrolysis of Polystyrene in Presence of Oxygen, Ionization Energy 100eV, Relative Intensity as Percentage of Base Peak 104.

m/e	Rel. Int.
14	128
16	*
18	169
26	25
27	30
28	*
29	25
32	*
34	14
39	28
40	25
44	30
50	53
51	80
52	30
63	14
65	8
74	19
77	44
78	70
91	9
103	47
104	100
105	22

*Off scale.

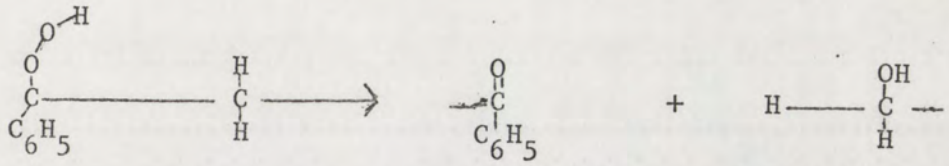

Grassie and Kerr[24] have reported similar degradation experiments at about 300°C and noted the formation of these products. Keto and hydroxyl groups were not detected in this study although the very intense O_2 peak at m/e = 32 may have masked the presence of CH_3OH. The only peaks larger than those normally observed for polystyrene were attributed to CO_2 at m/e = 44 and the oxygen molecule O^{16} O^{18} at m/e = 34. These results indicate that pyrolysis of polymers in a reactive atmosphere at high pressures (0.1 Torr) show greater fragmentation than in a vacuum. Diffusion of the degradation products from the sample surface apparently is hindered by the inert atmosphere keeping the sample in the high thermal zone for a longer period. Alternatively, oxygen accelerates the degradation process and in either case, results show a pattern with more secondary reactions and cracking[25].

Pyrolysis of polystyrene in the presence of the N_2 showed the opposite effect. As shown in Table 5, the relative intensities of the principal styrene fragments (91, 78, 51) have been significantly suppressed. The most probable cause for this phenomenon is a "charge neutralization" process where the charged fragments detectable by the ion multiplier are neutralized by collisions with N_2 molecules. Saturation of the detector cannot account for this suppression phenomenon because response to the very high concentrations of N^+_2 and N^{++}_2 was normal.

TABLE 5

Analysis of Products from Laser Pyrolysis of Polystyrene in Presence of Nitrogen; Ionization Energy 100 ev, Relative Intensity as Percentage of Base Peak 104.

m/e	Rel. Int.
14	4750
16	700
18	2000
26	200
28	*
29	600
32	4200
34	50
40	500
44	100
50	50
51	50
52	50
63	50
78	100
91	150
104	100

*Off scale.

Polyethylene

The major fragments generated by laser degradation of polyethylene were propylene, m/e = 41, and propane, m/e = 43, as shown in Table 6. On the other hand, mass spectrometric analysis of vacuum pyrolysis of polyethylene at temperatures from 335°C to 450°C by Madorsky and Straus[26] indicate butene m/e = 56 and butane m/e = 58 are the major pyrolysis fragments corresponding to 24.6 and 19.1 mole percent. In this study it would appear that the greater fragmentation was caused by a higher temperature at the sample surface. Principal mass peaks in the spectrum shown in Figure 9 indicate close correspondence to the empirical formula of polyethylene $(CH_2)_n$.

The presence of the background air spectrum was a definite disadvantage because of the N and N_2 at m/e = 14 and 28 mask the monomer CH_2, m/e = 14 and C_2H_4, m/e = 28 peaks. Comparison with the background spectrum taken before laser pyrolysis of polyethylene shows the relative intensity of m/e = 14 in Figure 21 to be about 5% greater than the background peak at m/e = 14, thus indicating the possible presence of the monomer CH_2.

On pyrolysis in a vacuum at temperatures up to about 500°C polyethylene decomposes to yield a spectrum of hydrocarbon fragments, saturated and unsaturated, varying in molecular weight from 16 to about 1000[25]. Compared to polystyrene, polyethylene yields less than 5% monomer, precluding an unzipping mechanism. The thermal degradation process of polyethylene is primarily random since all the C-C bonds have the same strength except for the few C-C bonds adjacent to tertiary carbon atoms occurring at branch points of the polymer. Madorsky and Straus[26] suggested a mechanism

TABLE 6

Mass Spectral Analysis of Principal Products from Laser Pyrolysis of Polyethylene in Vacuum, Ionization Energy 100 ev.

m/e	Rel. Int.*				
	Expt.	1	2	3	Rel. Dev. %
27		50	54	51	3.1
29		58	60	60	1.5
39		40	47	44	5.5
41		100	100	100	0
43		95	95	100	2.3
55		61	67	66	3.7
56		52	51	59	6.1
57		63	67	68	3.0
69		31	41	36	9.2
70		31	40	36	8.7
71		31	41	36	9.2
83		26	29	31	5.9
97		18	27	23	7.3
111		14.5	18	21	1.2
125		16.5	21	11	1.9
139		4.7	6	4	1.4

*Relative Intensity as a percentage of m/e = 41.

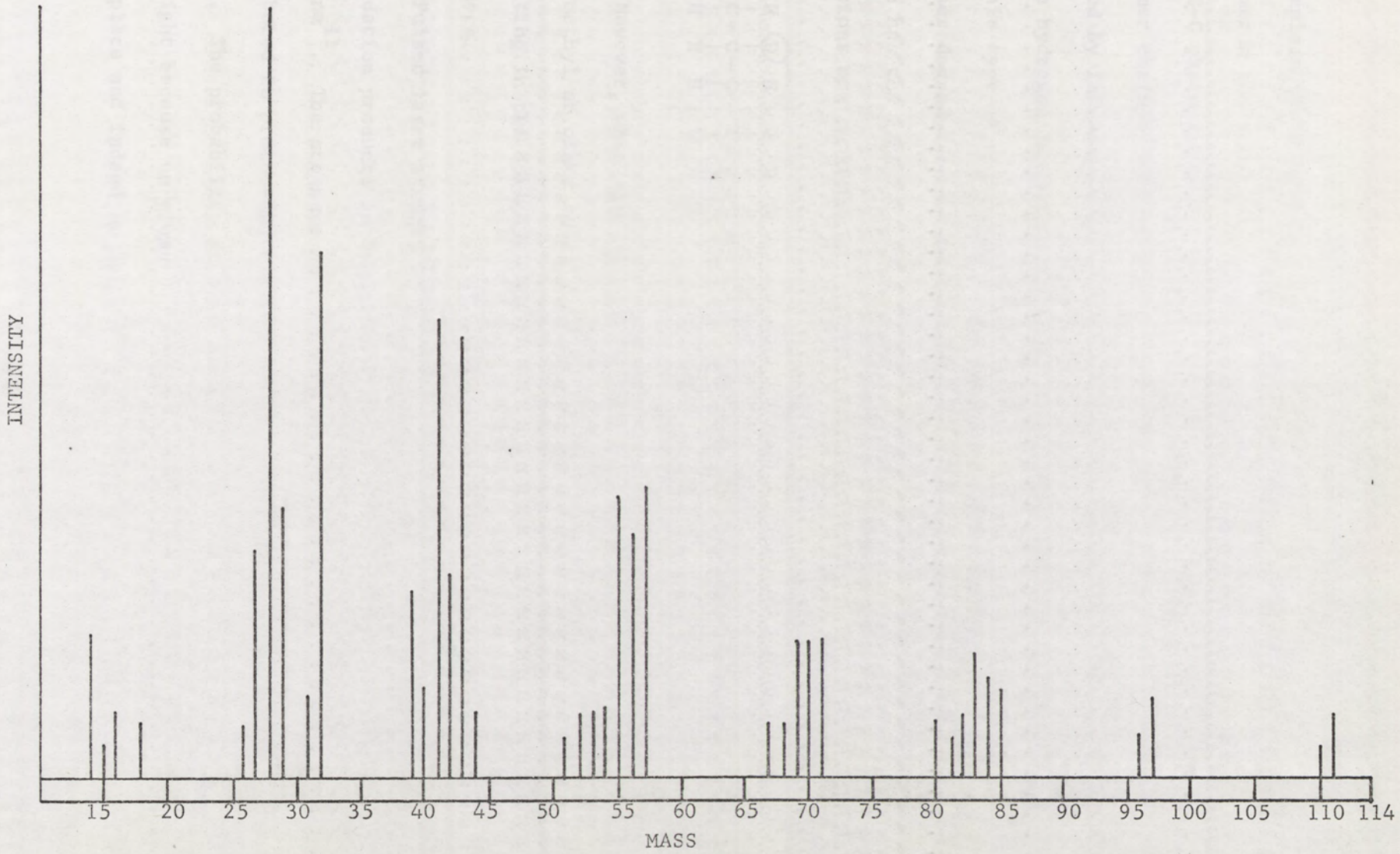

Figure 9. Mass spectrum of polyethylene obtained under continuous laser pyrolysis.

to explain their experimental results and the presence or absence of monomer in the pyrolysis of polystyrene and polyethylene in which most of the C-C chain scissions are caused by thermal stresses generated in the polymer chain by strong molecular vibrations. These scissions are accompanied by intramolecular hydrogen transfer at the site of the scissions where hydrogen is abundantly available, such is the case in polyethylene. In this type of scission, no free radicals are formed and therefore, no further degradation to monomers ensues. In the case of polyethylene, which has the greatest percentage of hydrogen of all organic polymers, the scissions are as follows:

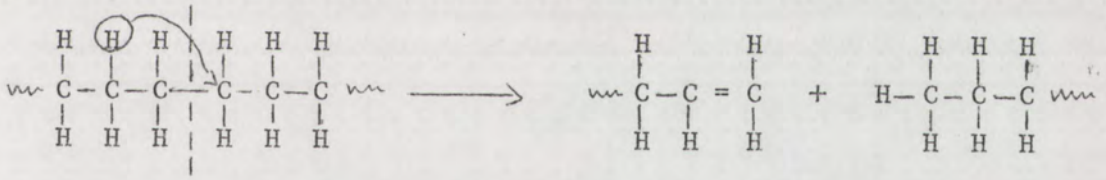

However, when some of the hydrogen atoms on the chain are replaced with methyl or other small groups, hydrogen transfer becomes hindered resulting in the formation of free radicals which can unzip to yield monomers.

Pulsed laser studies of polyethylene report the low molecular weight degradation products to be methane, ethane, ethylene, acetylene and propane[11]. The presence of methane (about 8% of the fraction) may be attributed to proton-CH_2 recombination in the high temperature laser plume. The probability of methane formation under continuous irradiation is slight because no plume is formed in which recombination reactions could take place and indeed no methane was detected in this investigation.

Methacrylate Polymers

The results of laser degradation studies of polymethylmethacrylate PMMA, polyethylmethacrylate PEMA, and polybutylmethacrylate PBMA, are given in Table 7. These results were very interesting because little or no monomer was detected, although other pyrolysis studies using conventional methods in the temperature range from 150°-500°C yields over 90% monomer[27]. The great predominance of monomer can be explained by the same mechanism previously suggested for polyethylene. Degradation takes place by random scissions, however in this polymer the scissions are not accompanied by hydrogen transfer at the site of the scission because of steric hindrance of the CH_3 and $COOCH_3$ groups at every alternate carbon. As shown below, the scissions result in the formation of free radicals.

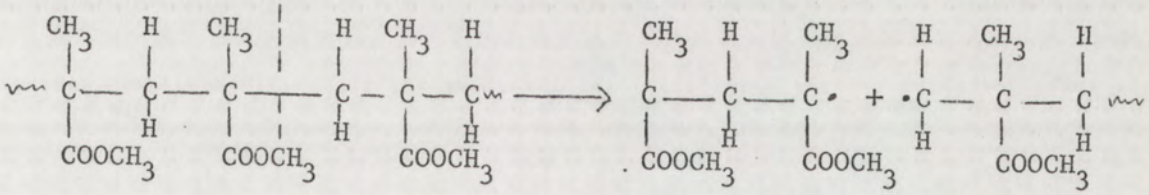

The free radicals then unzip to yield monomers:

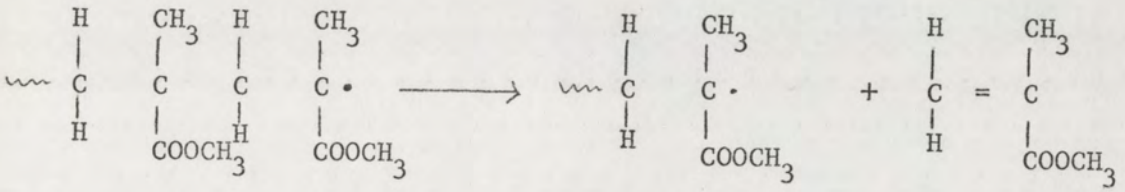

In consideration of the bulkier ethyl and butyl groups of PEMA and PBMA one would expect almost 100% monomer. However, the results of this study indicate little or no monomer for either PMMA, PEMA or PBMA.

Missing page 46

TABLE 7 (con't.)

	PBMA			
	Rel. Int.***			
m/e	Expt.	1	2	Rel.Dev. %
14		41	25	24
41		138	125	5
44		157	150	2.3
59		63	75	8.7
73		281	367	13.3
96		190	175	4.1
128		100	100	0
208		589	625	3
284		129	150	7.5

*** Relative intensity as percentage of monomer peak 128.

The explanation of these results can be found in a study by Lehmann and Brauer[28]. They conducted a series of experiments on high-temperature vacuum pyrolysis of PMMA using conventional methods and anlayzed the volatile products by gas chromatography. Over the temperature range from 425°-1025°C the amount of monomer decreased from 99 to 19.9%. Thus it would appear that, here, the surface temperature of the methacrylate samples were well in excess of 1000°C; this higher temperature caused greater fragmentation of degradation products with the resultant decrease in monomer.

2. PULSED IRRADIATION STUDIES

Polystyrene

Results from a study of appearance potentials of polystyrene monomer and benzene derived from the monomer are shown in Figure 10. As electron energy increases, the excess energy of the monomer will reach a value sufficient to break the weakest bond within the molecule and fragmentation results. This process continues with increasing probability until at about 23 ev the monomer intensity tends to reach a constant value. In conventional mass spectrometric work the energy required to produce the onset of the fragment ion is termed the appearance potential. However, in this study the fragment ion, benzene, was also produced by laser degradation at the sample surface. This section explores the consequences and possibilities of this process.

Ions produced by pulsed laser radiation have been reported by Knox[29] and Lincoln[30]. These experiments used a pulsed laser source and positioned

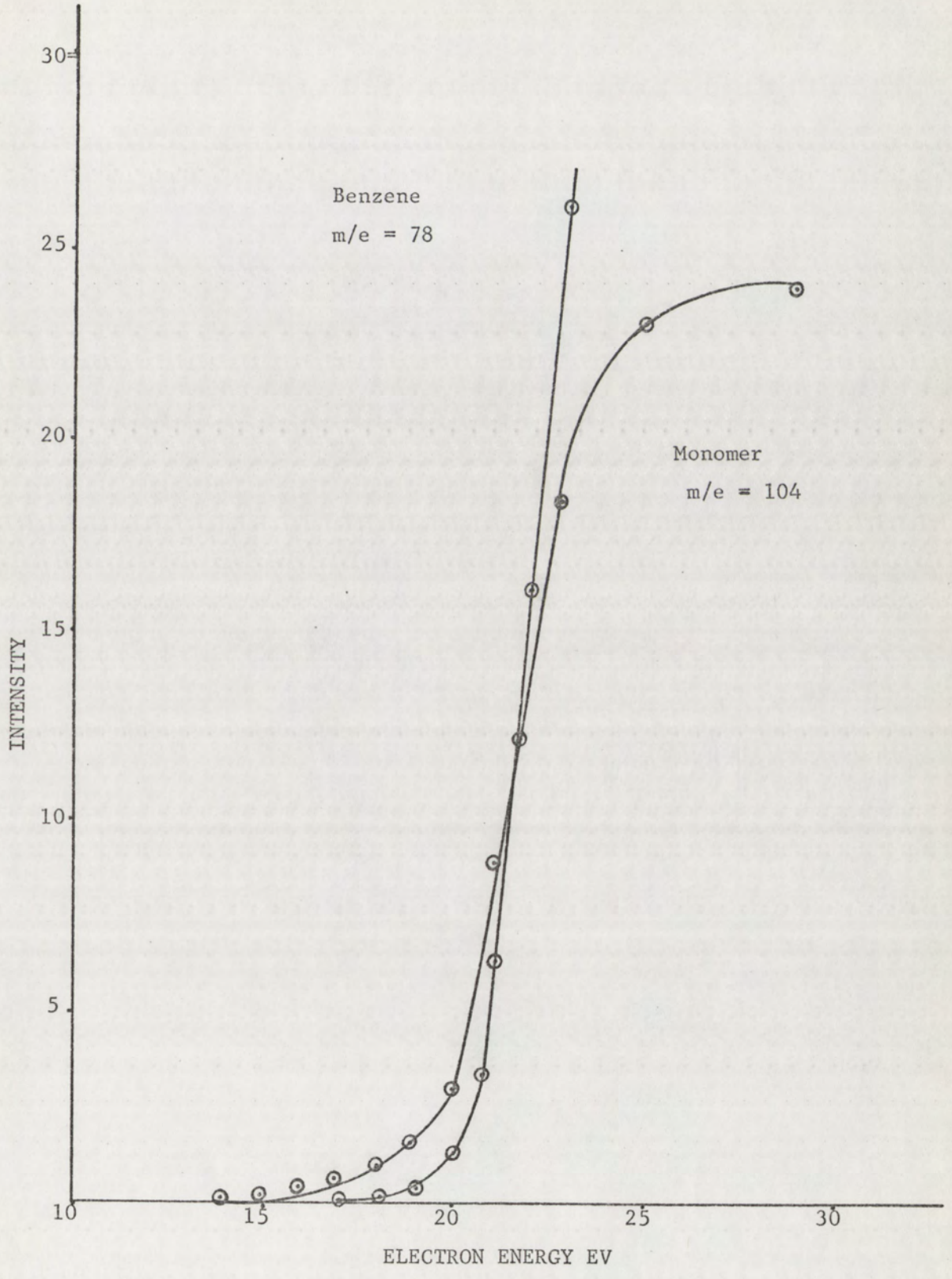

Figure 10. Electron ionization energy of monomer and benzene ion of polystyrene.

the sample within the drift tube and detector. The electron beam was switched off and ions produced directly by laser irradiation were detected. Experimental conditions in this study were somewhat different. The sample was placed 3 cm. below the ion source and ions produced directly from the thermal event could only be detected using highest sensitivity and maximum laser power. This is so since most of the ionic species would not be seen within the ion source but would deposit on metallic surfaces at ground potential before reaching the accelerating grids. Benzene and monomer ion fragments produced directly by the shuttered cw laser beam were detected at an energy deposition of 1.52 joules with a pulse duration of 0.19 sec. These experiments accomplished with the secondary fragmentation source, the ion beam, switched off demonstrate that the focused laser beam has sufficient energy to cause ionization at the sample surface. Time resolution of these two peaks showed the monomer component m/e = 104 reached maximum intensity 0.35 sec. after termination of the laser pulse followed by the benzene component with maximum intensity at 0.40 sec.

Due to this behavior, polystyrene monomer, the six-carbon fragment and the two-carbon fragment were selected for time-resolved studies based on the following decomposition model (here C_6H_6, shown as benzene for convenience, represents a six-carbon fragment while $C_2H_3^+$ is a two-carbon fragment denoted, for convenience, as et hylene):

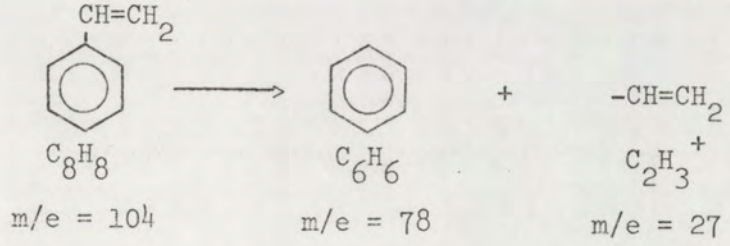

TABLE 8

Intensity of Polystyrene Monomer m/e = 104, Benzene m/e = 78, and Ethylene m/e = 27 as a Function of Laser Power and Deposition Time.

Deposition Time (sec.)	Deposition Energy (joules)	Intensity m/e = 27	Intensity m/e = 78	Intensity m/e = 104
		LASER POWER 3.5 watts		
0.20	0.7	-	-	2
0.21	0.7	-	-	2
0.22	0.8	1	2	14
0.85	3.0	5	12	76
0.86	2.0	6	10	83
		LASER POWER 5 watts		
0.05	0.3	-	-	-
0.20	1.0	3	4	19
0.22	1.1	1	1	4
0.23	1.1	4	12	21
0.25	1.3	7	15	34
0.56	2.8	16	28	65*
0.59	2.9	22	38	63*
1.03	5.1	15	24	64*
		LASER POWER 6 watts		
0.22	1.3	4	11	24
0.23	1.3	5	20	39
0.23	1.4	5	18	41
0.24	1.4	-	40	64
0.24	1.4	9	29	52
0.37	2.2	23	54	101
0.38	2.3	21	54	110
0.38	2.3	23	55	105
0.57	3.4	24	53	103*
		LASER POWER 7.2 watts		
0.05	0.4	.5	-	.5
0.075	0.5	-	20	53
0.14	1.0	32	30	59
0.15	1.1	36	35	63
0.20	1.4	34	34	63*
0.27	1.9	31	37	62*

TABLE 8 (con't.)

Deposition Time (sec.)	Deposition Energy (joules)	Intensity m/e = 27	Intensity m/e = 78	Intensity m/e = 104
		LASER POWER 7.9 watts		
0.06	0.5	-		
0.08	0.6	18	34	86
0.18	1.4	39	31*	53*
0.19	1.5	38	18	67
0.29	2.3	37*	28*	50*
0.29	2.3	34	40	60
0.61	4.8	29	34*	72*
0.63	5.0	32	40*	71*
0.64**	5.0	13*	22*	49*
0.66**	5.2	37*	40*	62*
1.02**	8.0	32*	26*	33*

*Indicates appearance of two maxima.

**Hole burned through sample.

The resultant intensity of monomer, benzene and ethylene as a function of laser power and pulse width are shown in Table 8. Some time resolved studies of particular m/e traces show double peaks and are denoted in Table 8 with an asterisk. Analysis of these data show that the threshold for the appearance of the double maxima is an energy deposition of at least 1.2 joules with minimum pulse width of 0.2 sec.

Figure 11 shows a representative trace of such a degradation with the ionization energy set at 100 ev. The trace for each component is binodal with maxima occurring both during and after the laser pulse. During the heating cycle, the monomer, m/e = 104, reaches a maximum slightly before benzene m/e = 78, followed in turn by the ethylene fragment. Shortly after termination of the laser pulse, ethylene achieves a second maximum followed in turn by the maxima of benzene and monomer. In all cases where the component peaks were well defined, as in Figure 11, the monomer peak occurred first followed by the peaks of benzene and ethylene. The different appearance times can only be explained by assuming that part of the degradation process is occurring on the sample surface. As the sample surface is heated, the temperature rapidly rises to a point where monomer is evolved. The thermal event continues and the surface temperature reaches a point where the monomer begins to decompose and its intensity declines with a corresponding increase in the benzene and ethylene fragments. Next, the benzene reaches peak intensity and then ethylene reaches maximum intensity shortly before the laser pulse is terminated. Upon completion of the laser pulse the sample cools and first passes through the temperature region where the ethylene fragment predominates

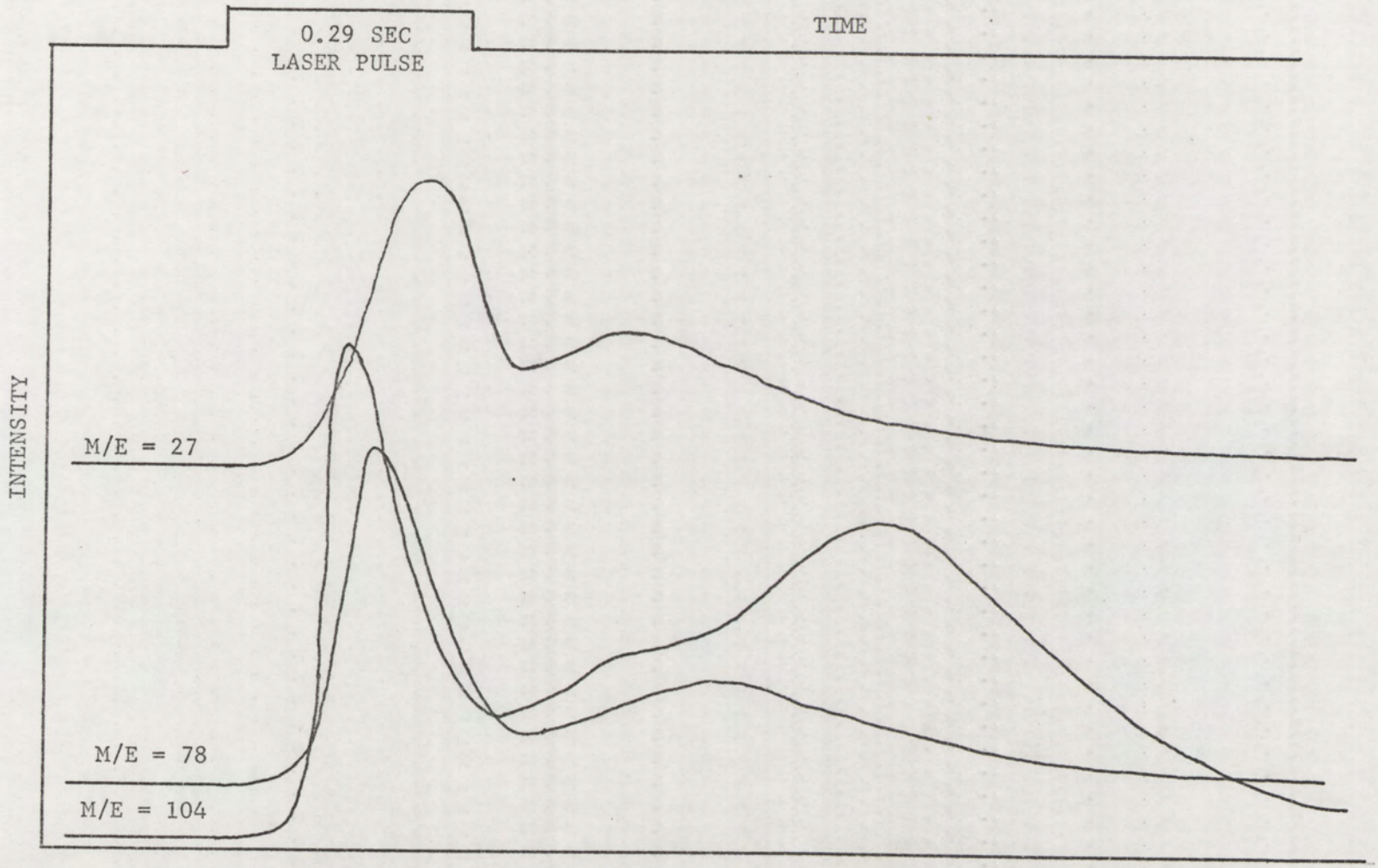

Figure 11. Time resolved study of ethylene m/e = 27, benzene m/e = 78 and styrene m/e = 104 from laser degradation of polystyrene. Laser power 7.9 watts.

and again the intensity of this fragment rises to a maximum. In a similar manner the continued decrease in temperature gives a broad peak for the benzene component followed by a broad peak for the monomer. In the cooling phase the peaks are broader because the rate of temperature change is much slower than during heating. A qualitative graphical description of this process is shown in Figure 12.

This type of behavior is only evidenced using intense thermal fluxes. The binodal traces of monomer, benzene, and ethylene shown in Figure 13 show another example of this process. At lower energy deposition rates, as shown in Figure 14, the intensity of benzene follows the monomer intensity, i.e. both exhibit the same time-intensity relationship. This suggests that benzene is derived from fragmentation of the monomer in the ion source and that only monomer is formed at the sample surface under these less severe conditions. This conclusion is consistent with the assumption of lower sample temperature, with no degradation of the sample beyond the monomer stage.

Other time resolved spectra showed evidence of burning a hole directly through the sample. This was evident by examination of the sample after a series of irradiations. Figure 15 shows a typical result. With the onset of the laser pulse a hole is quickly burned through the sample after which the laser beam strikes the stainless steel sample cup and reflects back into the sample. The plateau exists until the reflected beam has deposited sufficient energy to again raise the sample temperature to effect decomposition. The rapid increase of component intensities similar to Figure 11 and 13 is then evidenced.

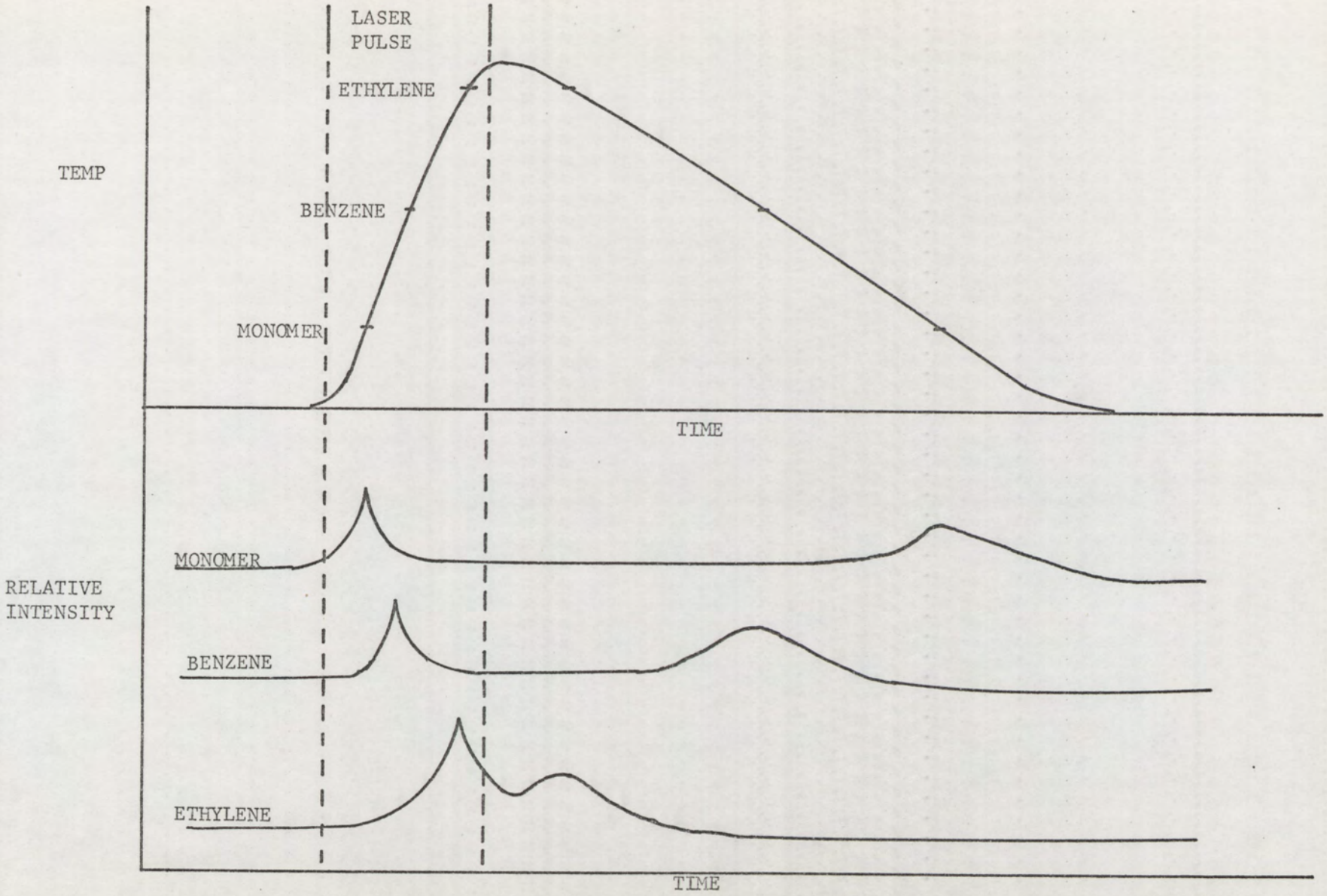

Figure 12. Graphical description of pulsed laser event.

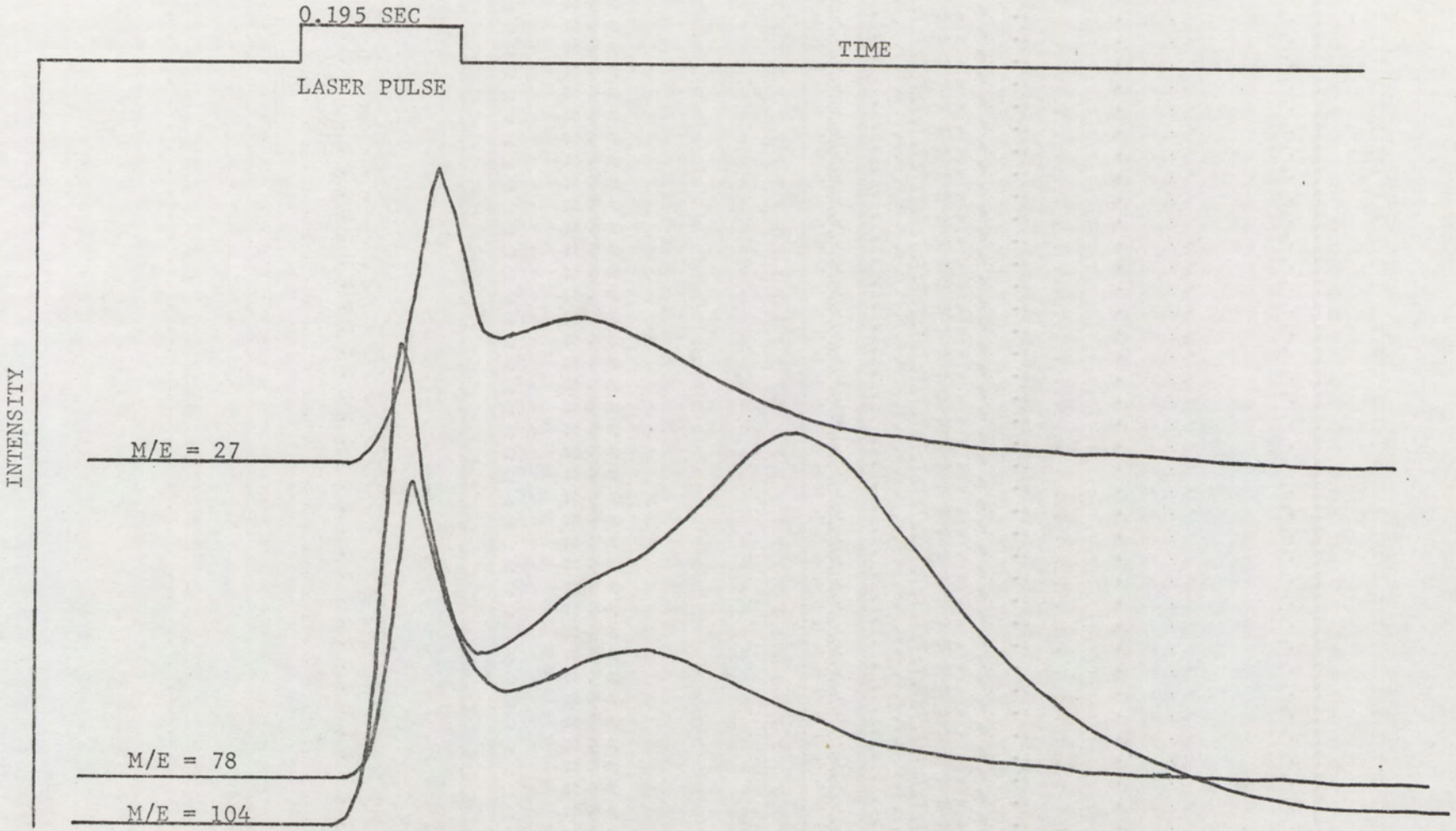

Figure 13. Time resolved study of ethylene m/e = 27, benzene m/e = 78 and styrene m/e - 104 from laser degradation of polystyrene. Laser power 7.9 watts.

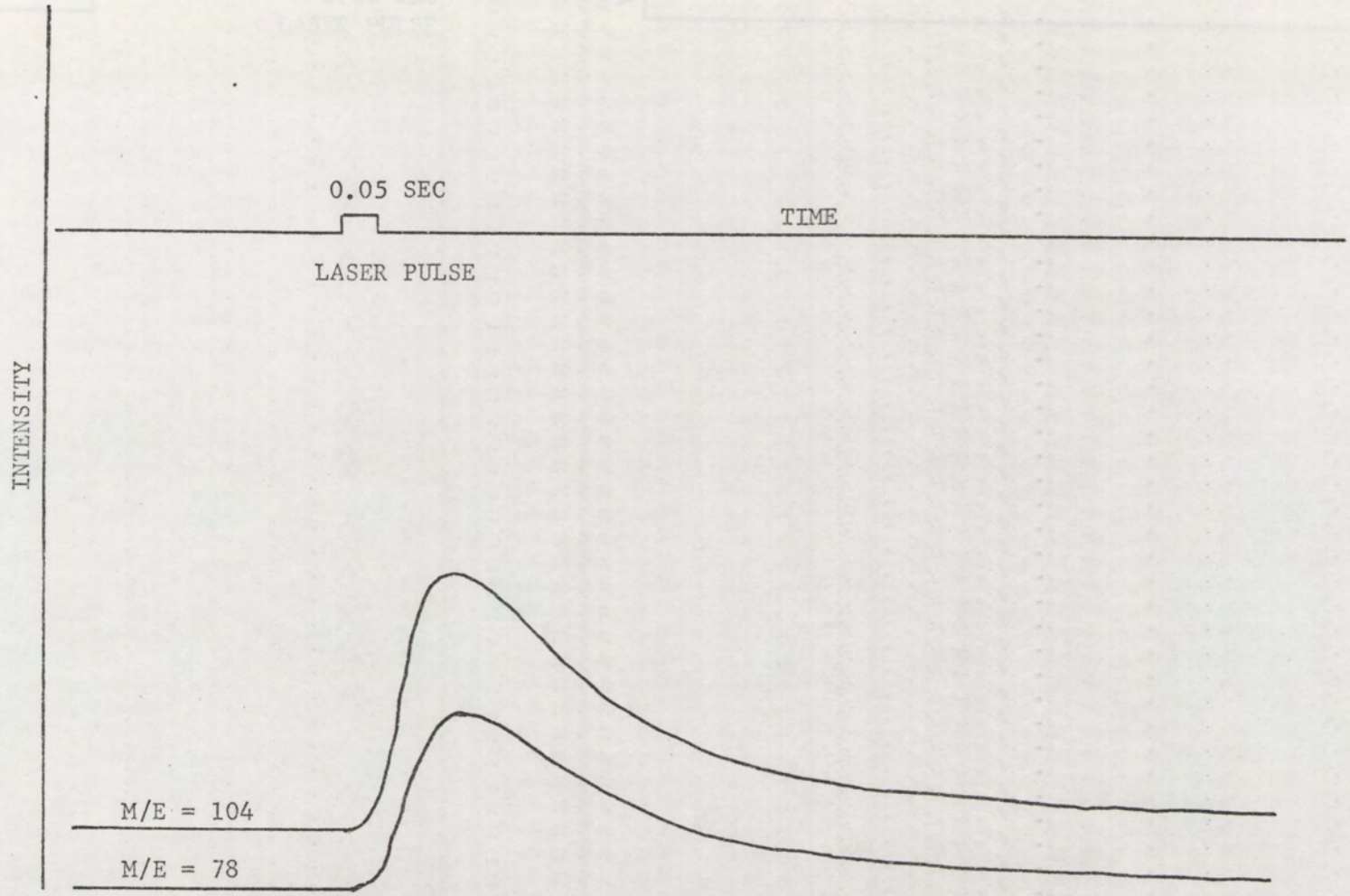

Figure 14. Time resolved study of benzene m/e = 78 and styrene m/e = 104 from laser degradation of polystyrene. Laser power 4.5 watts.

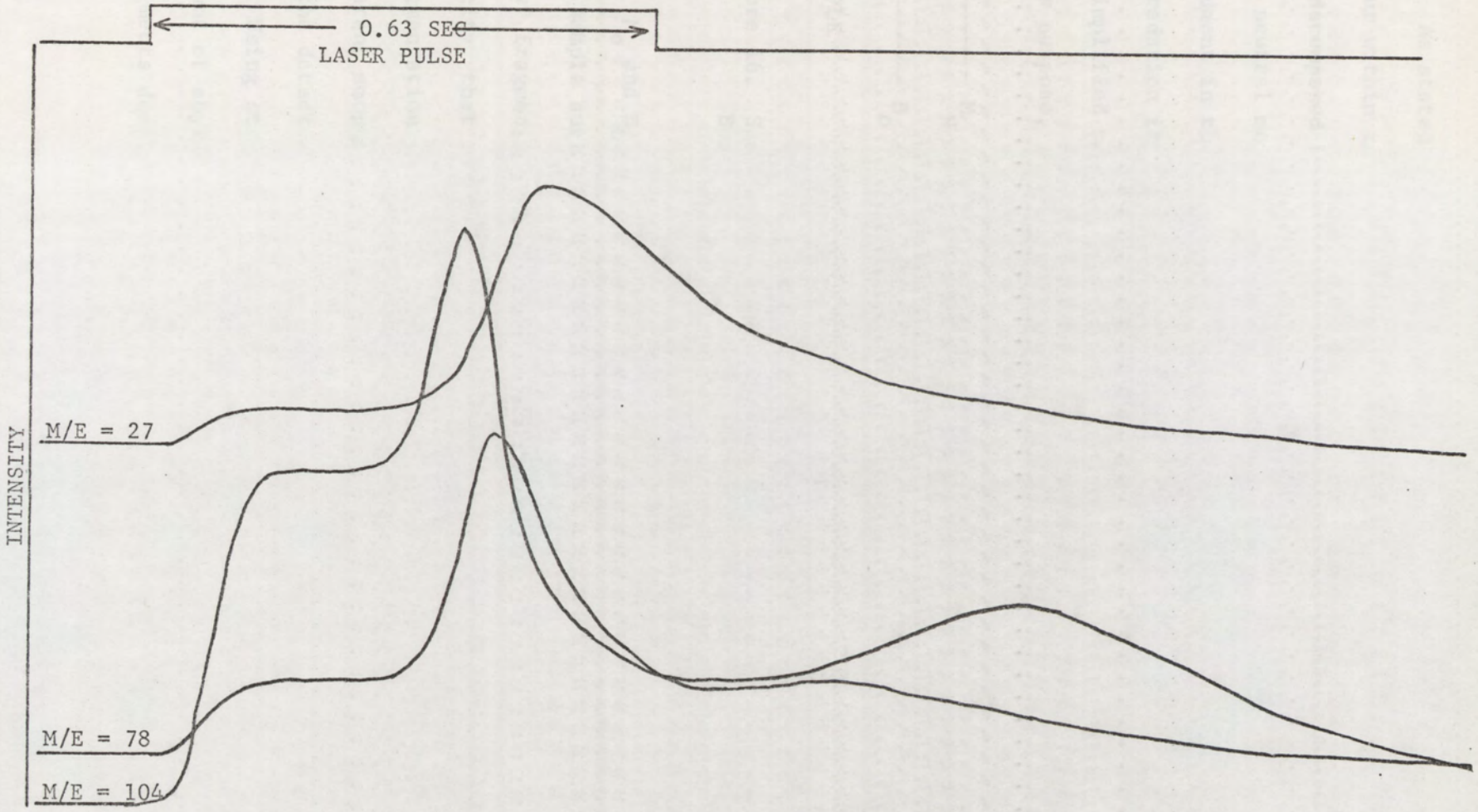

Figure 15. Time resolved study of ethylene m/e = 27, benzene m/e = 78 and styrene m/e = 104 from laser degradation of polystyrene at laser power of 7.9 watts. Sample burn through occurred.

As stated previously, there are two fragmentation processes that occur within the laser-mass spectrometer system. The sample material is decomposed by laser pyrolysis and these particles (ions, radicals, and neutral molecules) undergo further fragmentation upon electron bombardment in the ion source. In order to characterize the rate of thermal degradation it is necessary to distinguish between these two processes. A simplified model of the degradation ionization process, developed for this purpose, is shown in Figure 16.

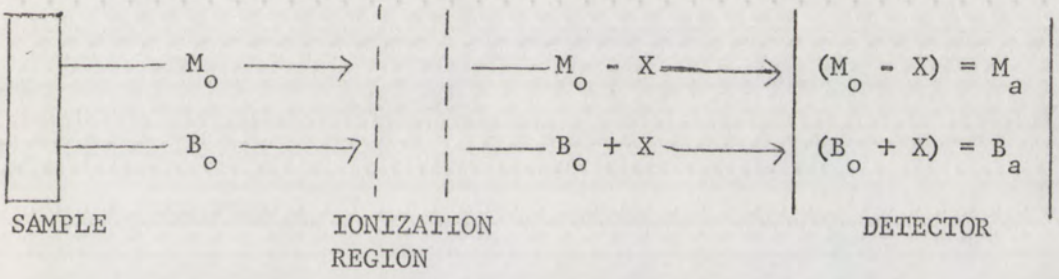

Figure 16. Simplified Degradation-Ionization Model of Monomer (M_o) and Benzene (B_o) Derived from Polystyrene.

M_o and B_o are the initial amounts of monomer and benzene formed at the sample surface during laser deposition. Although there are several other fragments formed upon decomposition of styrene, we assume, for simplicity, that within the ionization region only monomer M_o undergoes fragmentation by an amount X to form only benzene. M_a and B_a are the apparent amount of monomer and the apparent amount of benzene measured by the detector.

Using standard mass spectral tables, it is possible to estimate the amount of styrene M_o initially present considering the intensity of those fragments derived directly from styrene. This approach is quite approximate

although the components considered here are the predominate ones. The principal components in the conventional mass spectrum of styrene are styrene, M_a, benzene B_a, and a 4-carbon fragment C_4, with relative intensities of 100, 32.2 and 29.8 respectively[31]. Assuming B_a and C_4 are derived directly from styrene, the initial amount of monomer present may be written as the sum of these components.

$$M_o = M_a + B_a + C_4 \tag{4}$$

Considering the normal cracking patterns, M_o can be written in terms of M_a.

$$M_o = 1.62\ M_a \tag{5}$$

In the conventional cracking pattern of styrene, all benzene must be derived from styrene. The fraction of styrene converted to benzene within the ion source can therefore be determined from equation 6.

$$B_a = k_1 M_o \tag{6}$$

This leads to:

$$k_1 = \frac{B_a}{M_o} = \frac{0.322}{1.62} = 0.20 \tag{7}$$

Therefore, the fraction of benzene produced by ionization can be written as:

$$X = 0.20\ M_o \tag{8}$$

From the model in Figure 16, the benzene measured by the detector is given as:

$$B_a = (B_o + X) \tag{9}$$

Solving for B_o and substituting equations 8 and 5 for X, the initial amount of benzene B_o formed at the sample surface can be written as:

$$B_o = B_a - .32\ M_a \tag{10}$$

Within the assumptions previously stated it is now possible to calculate the amount of monomer and benzene produced from the sample with respect to time. Figure 11 was analyzed using equations 5 and 10 to calculate the monomer M_o and benzene B_o formed with respect to time at the sample surface. These parameters are shown in Figure 17.

The monomer M_o and benzene B_o curves of Figure 17 were graphically analyzed to determine the rate of change of each with respect to time. These data are tabulated in Appendix 1, Table 2. There is ample evidence from thermogravimetric experiments that polystyrene degradations follow first order kinetics[25]. The rate of product formation should be given by:

$$\frac{dI}{dt} = kI \tag{11}$$

where I is the amount of the degradation product, k is the specific rate constant and P is the amount of polymer present. The rate of product formation was determined from the slope of the curve I with respect to time analyzed at various time

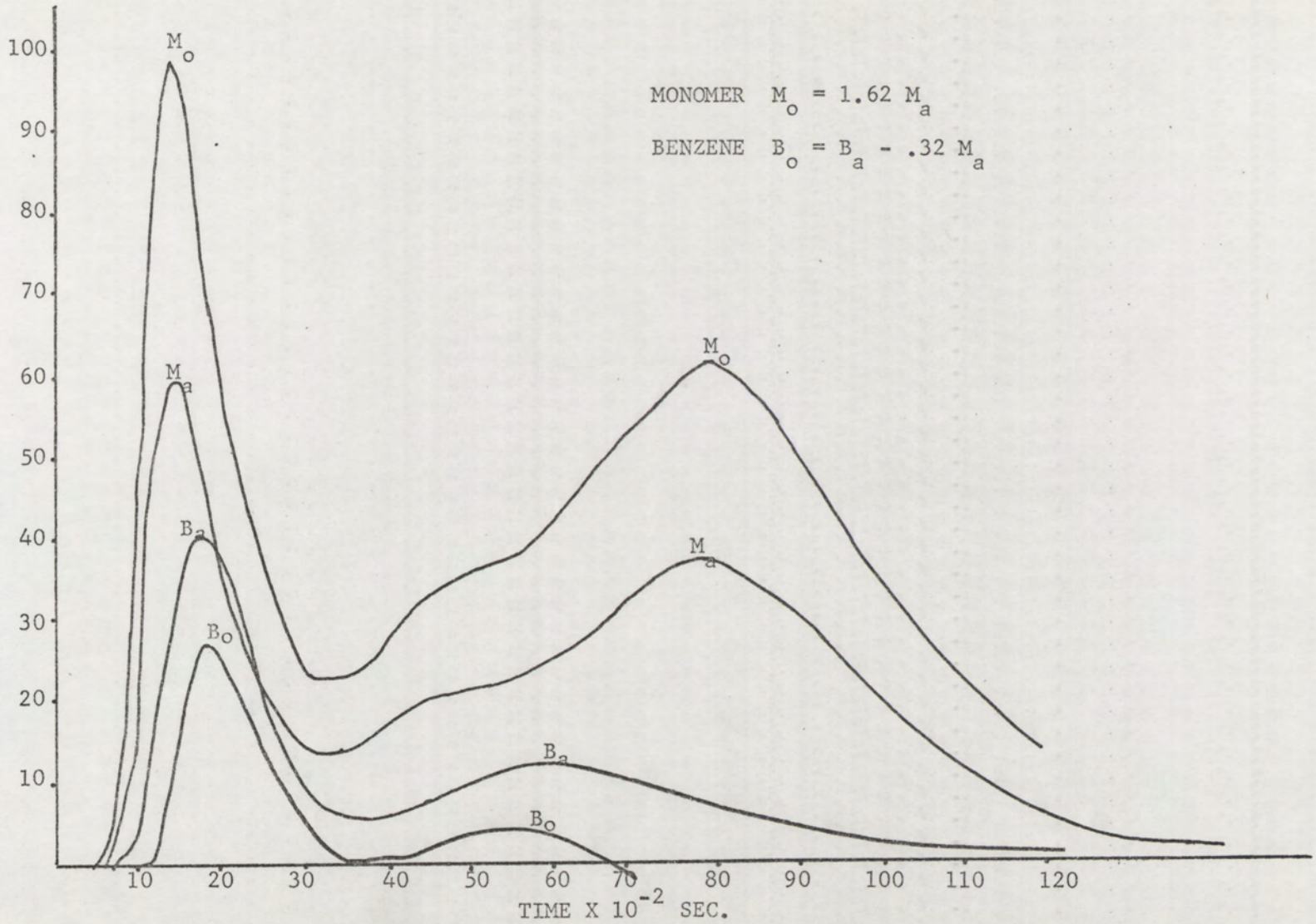

Figure 17. Intensity with respect to time for calculated monomer M_o and benzene B_o produced by laser pyrolysis only. M_a and B_a monomer and benzene actually detected.

intervals. Tangents were determined at five points on the upslope and five on the downslope of each trace. The upslope and downslope are defined respectively as those portions of the curve which are increasing and decreasing during the life time of the laser pulse.

Plots of the natural logarithm of intensity versus time for monomer and benzene produced by laser pyrolysis of polystyrene (Figure 11) are shown in Figures 18 and 19 respectively. The monomer indicates a linear relationship for both the upslope and downslope portions of the degradation curve. The benzene plot gives similar data although confidence in outlying data points is limited within the approximations of the model.

For comparison, a second time-resolved trace of laser produced polystyrene monomer and benzene were anlayzed as previously described to characterize the degradation rate. As shown in Figure 20 the laser pulse was of short duration (0.65 sec.) and the products reached maximum intensity after termination of the laser pulse. Plots of the natural logarithm of intensity versus time for the monomer and benzene are shown in Figures 21 and 22 respectively. Both the monomer and benzene plots again demonstrate the same general characteristics. The tabulated data for Figure 20 are contained in Appendix I, Table 3.

Although these degradation data show apparent first order behavior, they were not taken under isothermal conditions. Clearly, this is evidenced by equation 11 where I refers to the amount of polymer participating in the degradation reaction. These experiments degrade only a small fraction of the total sample and "I" must be considered for all purposes, essentially constant. Isothermal degradation conditions therefore would predict a

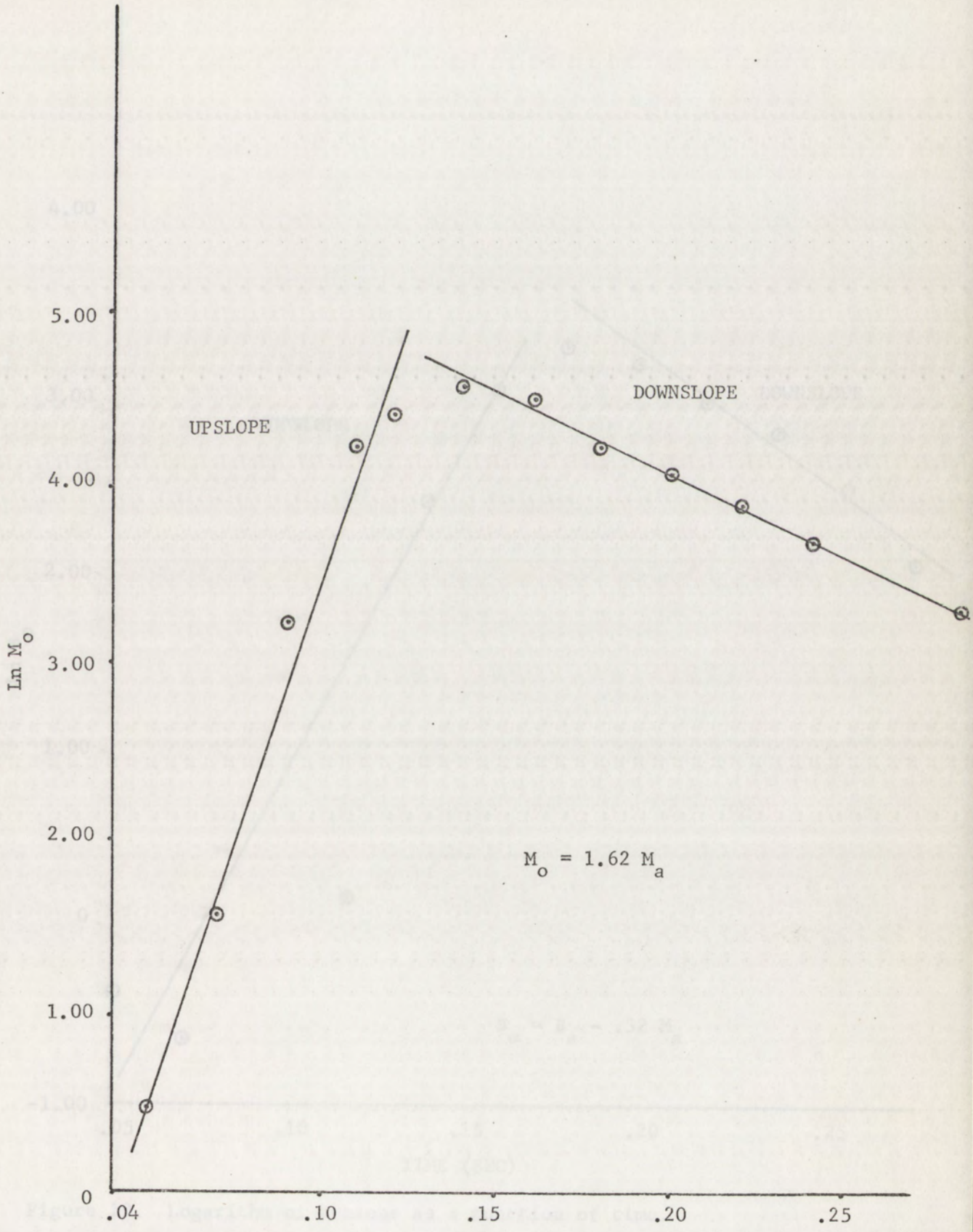

Figure 18. Logarithm of polystyrene monomer as a function of time.

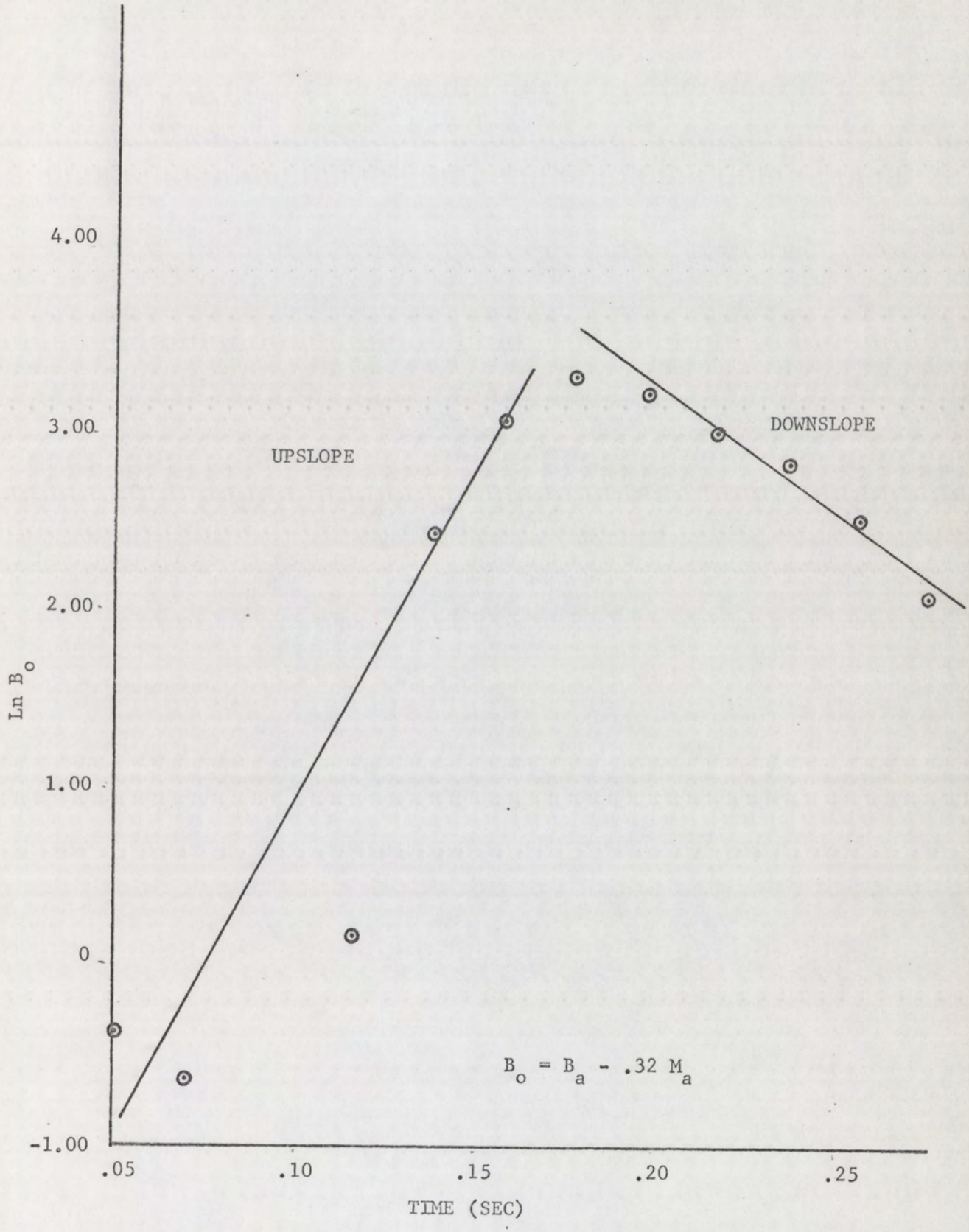

Figure 19. Logarithm of benzene as a function of time.

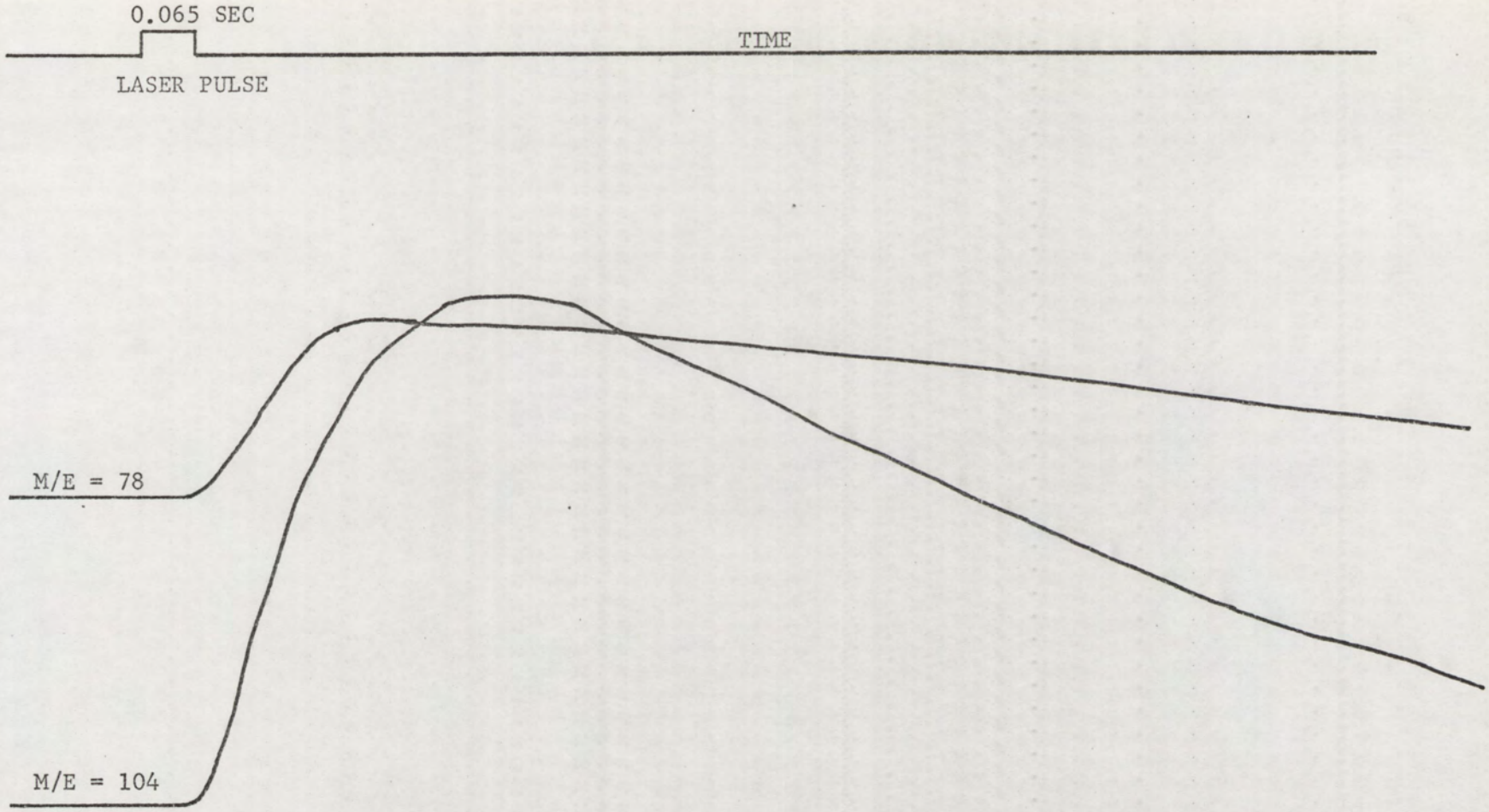

Figure 20. Time resolved study of benzene m/e = 78 and styrene m/e = 104 from laser degradation of polystyrene. Laser power 7.8 watts.

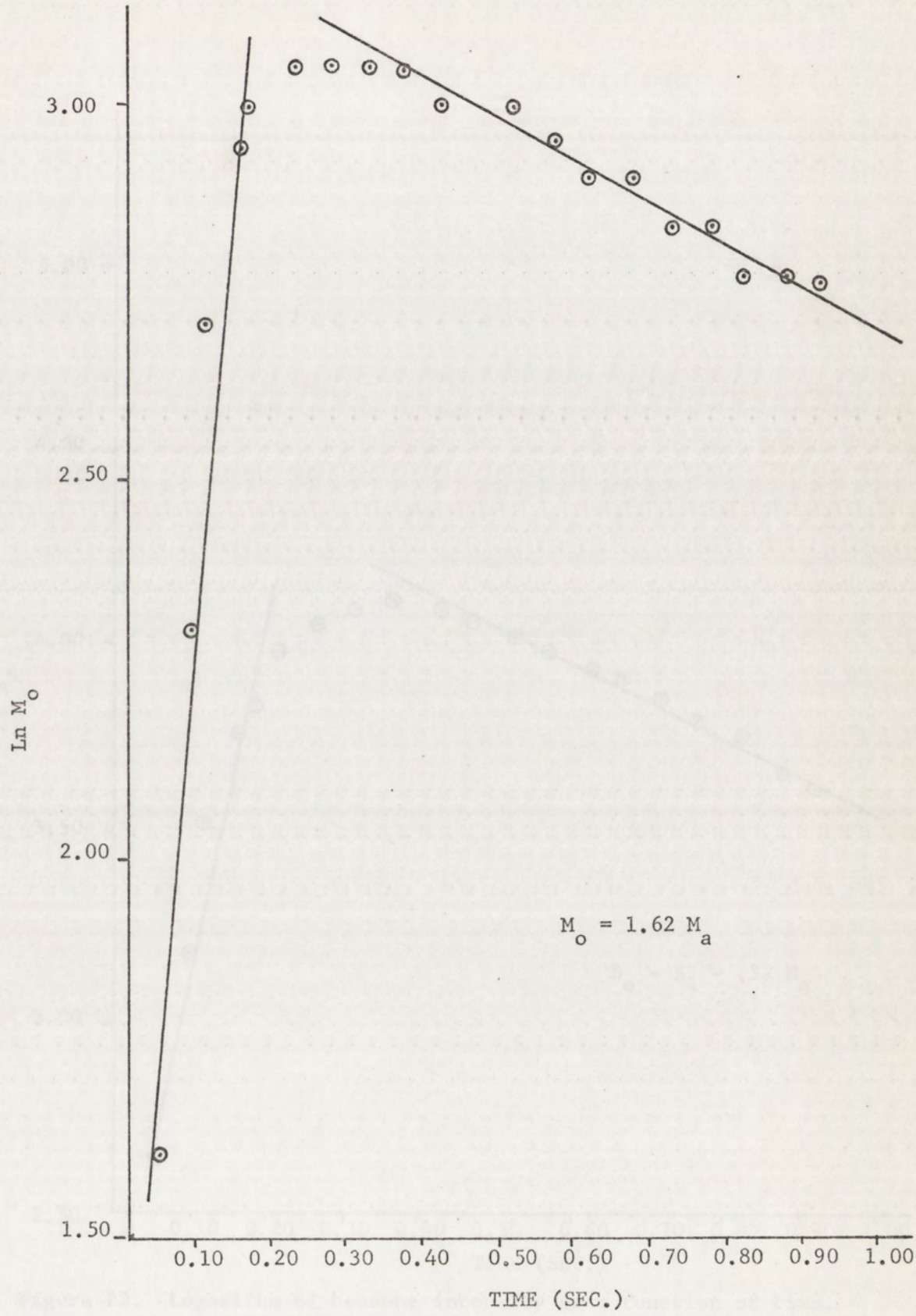

Figure 21. Logarithm of monomer intensity as a function of time.

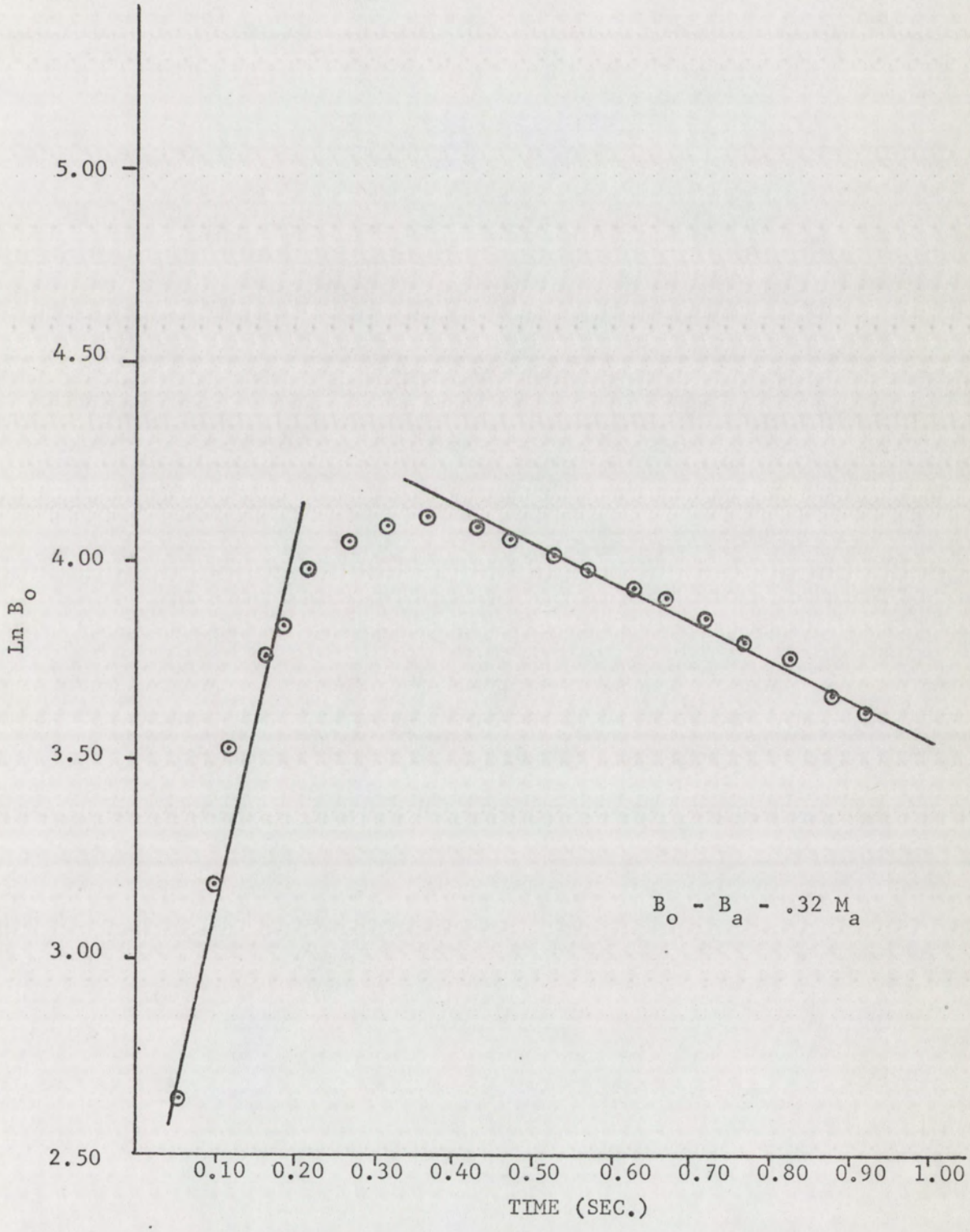

Figure 22. Logarithm of benzene intensity as a function of time.

constant rate of product formation. This is not found experimentally. In fact, the results clearly show that the sample temperature increases during the irradiation and these data can be used to estimate surface temperatures.

An estimate of reaction temperature was made by use of the Arrhenius equation:

$$k = Ae^{-E/RT} \tag{12}$$

where K is the specific rate constant at some absolute temperature T, A is the pre-exponential factor or Arrhenius factor, E is the activation energy and R is the gas constant. In logarithmic form equation 12 becomes

$$\ln k = \ln A^{-E/RT} \tag{13}$$

solving for T:

$$T = \frac{E}{R(\ln A - \ln k)} \tag{14}$$

Surface temperatures can be estimated from equation (15) for a specific value of k when the activation energy and the Arrhenius factor have been previously determined. In this instance k was determined by equation (11) as previously described and S. R. Urzendowski[33], using thermogravimetric analysis in vacuum at 370°-460°C, previously reported the activation energy and the Arrhenius factor of Cadco polystyrene to be 68.3×10^3 cal./mole and 2.3×10^{19} $sec.^{-1}$ respectively. The range of reaction

temperatures calculated for the monomer and benzene products in Figures 21 and 22 were 809-857^{o}K and 783-829^{o}K respectively. These temperature estimates are sensible and indicate that this approach has utility.

It is important to recognize the limitations of temperature estimates made with the Arrhenius Equation based on an activation energy which represents an average of the activation energies of all product molecules and taken at a temperature different from that determined by experimental data. Thus, it is not entirely valid to use an average value of activation energy with the rate constant of a specific product molecule to estimate temperatures. However, this error is reduced somewhat when a single degradation product predominates as is the case with polystyrene and methacrylate polymers.

CONCLUSION

Previous thermal degradation studies by many workers have very often been possibly only with large and time consuming analytical effort. More recent developments of instrumentation and techniques for rapid analysis include laser-mass spectrometer instruments similar to those used in this study. Although pulsed lasers have been used for sample pyrolysis within a mass spectrometer there are no prior reports of a continuous wave laser being used for this purpose.

Adaptation of the CO_2 laser and the time-of-flight instrument has shown that the combined instrumental technique is a valuable tool capable of rapid analysis and characterization of organic polymers.

The time-of-flight mass spectrometer is well suited for studies of fast reactions and transient phenomena due to its ability to present ten thousand mass spectra per second. The continuous wave CO_2 laser has proven to be a very good, although somewhat sophisticated, heat source for vaporization of solid samples. The focused beam of the CO_2 laser is highly desirable because the high surface temperatures are confined to the sample which acts as its own container and the small beam diameter limits the amount of sample vaporized. In addition, the study of ions generated directly by laser irradiation is possible by placement of small samples within the ion source in direct alignment with the drift tube.

This combined laser-time-of-flight instrument has expanded previous experimental capability of high energy (1-50 joules) and short deposition time (50 nsec. to 1 msec.) to include longer pulses (0.01 to 1 sec.) and lower energy deposition (0.1 to 3 joules). Operation in the continuous

mode has demonstrated that thermal degradation of polymers at high temperatures can be achieved with low power continuous wave lasers. Comparison of results obtained with this technique to those of conventional and pulsed laser degradation methods show close correspondence to conventional high temperature degradation studies.

The ability of the instrument to monitor individual fragments, permits time-resolved determination of reaction rate based on the formation of individual products. This permits more complete chemical description of the degradation processes and reaction rate than revealed by conventional methods such as thermogravimetric analysis where reaction rate is determined by the gross reaction parameter of weight loss with respect to time. Similarly, the activation energies determined by thermogravimetric analysis represent a proportionate average of the activation energies of all the products formed upon thermal decomposition. The study of these individual degradation products provides a far more complete description of the degradation mechanisms.

The time-resolved degradation studies of polystyrene show a definite temperature dependence on the type and amount of product formed. This temperature dependence of increased fragmentation at increasingly higher temperature was well evidenced by the order of appearance with respect to time of the maxima of styrene, benzene, and ethylene. The maxima of styrene always appeared first followed in turn by benzene and ethylene.

Repeated irradiations of the same sample altered the geometry of the exposed surface however, this had no adverse effects on the reproducibility of mass spectrograms even after 10 or more consecutive

exposures. Time-resolved studies of reaction rates were hampered by the additional fragmentation occurring from electron bombardment in the ion source and the mathematical model developed in this study was limited in accuracy by the simplifying assumptions of product fragmentation. However, rate studies of polystyrene using this model do show first order character consistent with the known reaction order of such decomposition reactions.

Schuddemage and Hummel[34], have demonstrated a field ionization method that nearly eliminates the secondary fragmentation characteristic of electron impact ion sources. In this method ionization takes place in the high voltage field of the platinum wire emitters resulting in very "gentle" ionization with almost every mass peak in the mass spectrogram arising only from a primary fragment of thermal decomposition. The field ionization source would be a very desirable improvement over the electron ion source for future degradation rate studies.

Characterization of degradation rates could also be improved by measurement of total ion current generated by the detector during the pulsed event. This would permit quantitative estimates of individual degradation products as a percentage of total ion current.

A 40-50 watt CO_2 laser would also improve experimental capability allowing greater energy deposition at times from 1 to 10 msec. Energy deposition with the 10 watt laser in this time regime was not sufficient to generate the binodal data observed at longer deposition times.

The versatile means to continuously pyrolyze samples from a remote source and rapidly analyze the degradation products will assure greater

use of this technique in the future.

APPENDIX

TABLE 1

Rate and Rate Constant Derived From Figure 17

Monomer

No.	Time t(sec)	Intensity I	ΔI	Δt	Rate $\frac{\Delta I}{\Delta t}$	k $\frac{I}{\text{rate}}$	Ink	Temp (^{o}K)
1	.09	6	78	0.10	780	130	4.87	857
2	.11	22	78	0.05	1560	71	4.26	845
3	.12	35	78	0.06	1300	37	3.61	832
4	.13	48	78	0.06	1300	27	3.30	825
5	.14	56	78	0.12	650	11.6	2.45	809

Benzene

1	.11	5	64	.13	493	98.5	4.59	852
2	.12	11	64	.12	533	48.4	3.88	837
3	.14	23	64	.10	640	27.8	3.32	846
4	.15	31	64	.08	800	25.8	3.25	825
5	.16	37	64	.14	457	12.4	2.52	810

TABLE 2

TIME-INTENSITY DATA DERIVED FROM FIGURE 17

No.	Time t(sec)	Benzene B_a	Monomer M_a	$.32M_a$	B_o $(B_a - .32M_a)$	M_o $(1.62M_a)$
1	.05	1	1	.32	.68	1.62
2	.07	1.5	3	.96	.54	4.9
3	.09	3	16	5.1	-2.1	25.9
4	.11	12.5	42	13.4	- .9	68
5	.12	17.5	51	16.3	1.2	83
6	.14	31	61	19.4	11.6	99
7	.16	40	57	18.2	21.8	92
8	.18	42	43	13.8	28.2	70
9	.20	37	37	11.8	25.2	60
10	.22	31	31	9.9	21.1	50
11	.24	25	25	8.0	17.0	40
12	.26	20	22	7.0	13.0	36
13	.28	14	18	5.8	8.2	29
14	.30	10	15	4.8	5.2	24
15	.34	6	15	4.8	1.2	24
16	.38	7	16	5.1	1.9	26
17	.42	8	19	6.1	1.9	31
18	.46	10	21	6.7	3.3	34
19	.50	12	22	7.1	4.9	36
20	.54	12	23	7.4	4.6	37
21	.58	12	25	8.0	4.0	40
22	.62	12	28	9.0	3	45
23	.66	11	31	9.9	1.1	50
24	.70	10	34	10.9	- .9	55
25	.74	9	36	11.5	-2.5	57
26	.78	8	38	12.1	-4.1	62
27	.82	7	37	11.8	-4.8	60
28	.86	5	35	11.2	-6.2	57

TABLE 2 (cont.)

No.	Time t(sec)	Benzene B_a	Monomer M_a	$.32M_a$	B_o $(B_a - .32M_a)$	M_o $(1.62M_a)$
29	.90	5	31	9.9	-4.9	50
30	.94	4	27	8.7	-4.7	44
31	.98	3.5	23.5	7.5	-4.0	38
32	1.02	3	20	6.4	-3.4	32
33	1.06	2	18	5.8	-3.8	29
34	1.10	2	13	4.2	-2.2	21
35	1.14	2	11	3.5	-2.5	18

TABLE 3

Time-Intensity Data Derived From Figure 20

No.	Time t(sec.)	Benzene B_a	Monomer M_a	B_o $(B_a - .32M_a)$	M_o $(1.62M_a)$
1	0.05	14	5	12.4	8.1
2	0.08	24	10	20.8	16.2
3	0.11	34	15	29.2	24.3
4	0.15	43	19	36.9	30.8
5	0.17	46	20	39.6	32.4
6	0.22	53	21	46.3	34
7	0.27	58	21	51.3	34
8	0.32	60	21	53.3	34
9	0.37	61	20	54.6	32.4
10	0.42	60	20	53.6	32.4
11	0.47	58	20	51.6	32.4
12	0.52	57	19	50.9	30.8
13	0.57	54	18	48.2	29.2
14	0.62	51	18	45.2	29.2
15	0.67	49	18	43.1	29.2
16	0.72	47	17	41.6	27.5
17	0.77	44	17	38.6	27.5
18	0.82	42	16	36.9	25.9
19	0.87	39	16	33.9	25.9
20	0.92	37	15	32.2	24.3

TABLE 4 .

Rate and Rate Constant Derived From Figure 20

Monomer

No.	Time t(sec)	Intensity I	ΔI	Δt (sec)	Rate $\frac{\Delta I}{\Delta t}$	K $\frac{\text{Rate}}{I}$	Temp (^{o}K)
1	0.05	5	38	0.25	152	30.9	829
2	0.08	10	38	0.25	152	15.2	819
3	0.11	15	43	0.30	143	9.5	809
4	0.15	19	60	0.84	71	3.7	792
5	0.17	20	48	1.03	47	2.4	783

Benzene

1	0.09	25	83	0.26	319	12.8	814
2	0.16	44	49	0.26	188.5	4.29	793
3	0.21	53	42	0.37	113.5	2.4	782
4	0.26	57	35	0.37	94.6	1.7	774
5	0.30	59	23	0.37	62.1	1.1	766

BIBLIOGRAPHY

1. Levy, R. L., "Pyrolysis Gas Chromatography: A Review of Technique," Chromatography Reviews 8, 48, 1966.

2. Madorsky, S. L., V. E. Hart, S. Strauss, Journal of Research, National Bureau of Standards 51, 329, 1953.

3. Madorsky, S. L., Thermal Degradation of Organic Polymers, P. 4, Interscience Publishers, 1964.

4. Berkowitz, J. and W. A. Chupka, "Mass Spectrometric Study of Vapor Ejected from Graphite and other Solids," Journal of Chemical Physics 40, 2735, 1964.

5. Chang, T. Y. and C. K. Birdsall, "Laser-Induced Emission of Electrons, Ions and Neutrals from Ti and Ti-D Surfaces," Applied Physics Letters, 5, 171, 1964.

6. Honig, R. E., "Laser-Induced Emission of Electrons and Positive Ions from Metals and Semiconductors," Applied Physics Letters 3, 8, 1963.

7. Lincoln, K. A., "Simple Display System for Recording Time-Resolved Mass Spectra," Review of Scientific Instruments 35, 1688, 1964.

8. Ready, J. F., "Development of Plume Material Vaporized by Giant-Pulse Laser," Applied Physics Letters 3, 11, 1963.

9. Ready, J. F., Journal of Applied Physics 36, 462, 1965.

10. Lincoln, K. A., "Mass Spectrometric Studies Applied to Laser-Induced Vaporization of Polymeric Materials," High Temperature Technology. Proceedings of the Third International Symposium, P. 323 Asilomar, California, 1967.

11. Ristau, W. T. and N. E. Vanderborgh, "Laser-Induced Degradation of Hydrocarbon Compounds Analyzed Using Gas-Liquid Chromatography," Analytical Chemistry, 43, 702, 1971.

12. Parts, L., "The Laser in Chemistry," Scientific Research 2, 46, 1967.

13. Lincoln, K. A., "Flash Vaporization of Solid Materials for Mass Spectrometric Analysis by Intense Thermal Radiation," Analytical Chemistry 37, 541, 1965.

14. Vastola, F. J., "Analysis fo Coal with Laser-Mass Spectrometer," American Chemical Society, Division of Fuel Chemistry, 11(4), 229, 1967.

15. Vastola, F. J., R. V. Mumma, A.J. Pirone, "Analysis of Organic Salts by Laser Irradiation," Organic Mass Spectrometry 3, 101,. 1970.

16. Knox, B. E. and V. S. Ban, "Mass Spectrometric Study of Laser-Induced Vapor of Compounds of Bi with Elements of Group VI A," Journal of Chemical Physics, 52, 243, 1970.

17. Knox, B. E. and V. S. Ban, "Mass Spectrometric Study of Laser-Induced Vaporization of As, and Sb Compounds with Elements of Groups VI A," Journal of Chemical Physics 52, 248, 1970.

18. Bernal, E. G., L. P. Levine and J. F. Ready, "Time of Flight Spectrometer for Laser Surface Interaction Studies," Review of Scientific Instruments 37, 938, 1966.

19. Biemann, K., Mass Spectrometry Organic Applications, McGraw-Hill Inc., New York, N Y., 1962.

20. Hodgman, C. D., Handbook of Chemistry and Physics, 31st Edition, Chemical Rubber Publishing Co., Cleveland, Ohio 1949.

21. McLafferty, F. W., Interpretation of Mass Spectra, W. A. Benjamin Inc., New York, New York, 1967.

22. Staudinger, H. M. Brunner, and K. Frey, Berichte, 62B, 241, 1929.

23. Jellinek, H. H. G., Journal of Polymer Science 3, 850, 1949.

24. Grassie, N. and W. W. Kerr, Trans. of Faraday Society 53, 234, 1956.

25. Madorsky, S. L., Thermal Degradation of Organic Polymers, Interscience Publishers, P. 93, 1964.

26. Madorsky, S. L., and S. Straus, Journal of Research, National Bureau of Standards, 53, 361, 1954.

27. Straus, S. and S. L. Madorsky, Journal of Research, National Bureau of Standards 66A, 401, 1962.

28. Lehman, F. A. and G. M. Brauer, Analytical Chemistry 33, 673, 1961.

29. Knox, B. E., "Molecularity and Charge States of Laser Vaporized Materials," Symposium on Thermokinetic Effects in Pulsed Energy Deposition, Albuquerque, New Mexico, Oct. 1970.

30. Lincoln, K. A., "Laser Induced Carbon Vaporization and Chemical Reactions," Symposium on Thermokinetic Effects in Pulsed Energy Deposition, Albuquerque, New Mexico, Oct. 1970.

31. Cornu, A. and R. Massot, Compilation of Mass Spectral Data, Heydon & Son Limited, Paris, France, 1960.

32. Patel, C. K. N., "High-Power Carbon Dioxide Lasers," Scientific American, 219, 22, August 1968.

33. Urzendowski, S. R., "A Thermogravimetric Study of the Kinetics of Polymer Pyrolysis," AFWLTR-69-46, Air Force Weapons Laboratory, Kirtland AFB, New Mexico, 1969.

34. Schuddemage, H. D. R. and D. O. Hummel, "Characterization of High Polymers by Pyrolysis within the Field Ionization Mass Spectrometer," Advances in Mass Spectrometry, Vol. 4, P. 857, Proceedings of a Conference held in Berlin, Sept. 1967.